Association analyses of host genetics, root-colonizing microbes, and plant phenotypes under different nitrogen conditions in maize

Michael A. Meier[1,2], Gen Xu[1,2], Martha G. Lopez-Guerrero[3], Guangyong Li[1,2], Christine Smith[2], Brandi Sigmon[4], Joshua R. Herr[2,4], James R. Alfano[2,4]*, Yufeng Ge[5], James C. Schnable[1,2,**] and Jinliang Yang[1,2,**]

[1]Department of Agronomy and Horticulture, University of Nebraska-Lincoln, Lincoln, NE 68583, USA.
[2]Center for Plant Science Innovation, University of Nebraska-Lincoln, Lincoln, NE 68583, USA.
[3]Department of Biochemistry, University of Nebraska-Lincoln, Lincoln, NE 68588, USA
[4]Department of Plant Pathology, University of Nebraska-Lincoln, Lincoln, NE 68583, USA.
[5]Biological Systems Engineering Department, University of Nebraska-Lincoln, Lincoln, NE 68583, USA

*Author JA is deceased at the time of publication.

**Correspondence may be addressed to:
jinliang.yang@unl.edu
schnable@unl.edu

Abstract

The root-associated microbiome (rhizobiome) affects plant health, stress tolerance, and nutrient use efficiency. However, it remains unclear to what extent the composition of the rhizobiome is governed by intraspecific variation in host plant genetics in the field and the degree to which host plant selection can reshape the composition of the rhizobiome. Here we quantify the rhizosphere microbial communities associated with a replicated diversity panel of 230 maize (*Zea mays L.*) genotypes grown in agronomically relevant conditions under high N (+N) and low N (-N) treatments. We analyze the maize rhizobiome in terms of 150 abundant and consistently reproducible microbial groups and we show that the abundance of many root-associated microbes is explainable by natural genetic variation in the host plant, with a greater proportion of microbial variance attributable to plant genetic variation in -N conditions. Population genetic approaches identify signatures of purifying selection in the maize genome associated with the abundance of several groups of microbes in the maize rhizobiome. Genome-wide association study was conducted using the abundance of microbial groups as rhizobiome traits, and identified n = 622 plant loci that are linked to the abundance of n = 104 microbial groups in the maize rhizosphere. In 62/104 cases, which is more than expected by chance, the abundance of these same microbial groups was correlated with variation in plant vigor indicators derived from high throughput phenotyping of the same field experiment. We provide comprehensive datasets about the three-way interaction of host genetics, microbe abundance, and plant performance under two N treatments to facilitate targeted experiments towards harnessing the full potential of root-associated microbial symbionts in maize production.

Introduction

Symbiotic relationships between plant hosts and root-associated microbes have been shaped through natural selection over millions of years of coevolution (Limborg and Heeb, 2018), and have been a driver of crop performance and yield in agricultural production since the beginning of plant domestication (Yadav et al., 2018). Microbial actors in the rhizosphere have been shown to promote plant growth (Saleem et al., 2019), improve nutrient use efficiency (Gomes et al., 2018; Zhu et al., 2016), and reduce abiotic stress response (Hussain et al., 2018). The promise of high throughput screens for plant growth promoting activity in isolated microbial strains or synthetic communities (Singer et al., 2021; Yee et al., 2021) is the potential discovery of microbial agents that can be used as seed or soil additives to improve crop performance under field conditions. Promising results have been observed in controlled environments (Van Gerrewey et al., 2020; Xi et al., 2020; Yu et al., 2021), but it remains a challenge to achieve similar outcomes in crops under agriculturally relevant field conditions (Eida et al., 2017; Kaur et al., 2020; Sessitsch et al., 2019). Many microbial inoculants struggle to compete with naturally occurring microbes in the rhizosphere and rarely survive for extended periods of time in the field (Piromyou et al., 2011). An improved understanding of how plants shape the composition of their rhizobiomes under diverse field conditions would make it more feasible to identify beneficial plant-microbe interactions that will be persistent and replicable in field environments. Moreover, studying the effects of plant genetics on microbial communities may identify opportunities to breed crop plants that recruit and maintain superior growth-conducive microbial communities from the natural environment.

Few studies to date have addressed the relationship between plant genetics and rhizobiomes in field settings, mainly because large-scale rhizosphere sampling (as opposed to leaf microbiome sampling) and DNA sequence analysis of microbial communities in diverse plant hosts is time-

consuming, expensive, and poses significant logistical and technical challenges. It has been shown that plant genetics can explain variation in both root architecture (Bray and Topp, 2018) and exudation (Mönchgesang et al., 2016). If these factors in turn shape microbial communities (Sasse et al., 2018), variation in the root-associated microbial groups (hereafter referred to as rhizobiome traits) may also result from genetic factors. Recent studies suggested that the variation in the composition of rhizobiomes is likely controlled by plant genetic factors (i.e., heritable) in maize (Peiffer et al., 2013), sorghum (Deng et al., 2021), and switchgrass (Sutherland et al., 2021). However, to what extent these heritable microbes are affected by the plant host and contribute to variation in the crop phenotype remains unclear. Like any other trait under heritable genetic control, rhizobiome traits can be targeted in selective breeding experiments. To explore this idea, previous efforts have been directed towards identifying plant genetic loci that are associated with rhizobiome traits. Initial studies have shown that rhizosphere microbial communities differ between distinct genotypes of the same host species, which has been shown in a study on 27 maize genotypes (Peiffer et al., 2013; Walters et al., 2018) and more recently, in a diversity panel of 200 sorghum lines (Deng et al., 2021). Genome-wide association study (GWAS) has successfully revealed associations between plant genes and rhizobiome traits at high-level measures of rhizosphere community dissimilarity (i.e., using principal components) in an *Arabidopsis* diversity panel (Bergelson et al., 2019) or at order level (derived from operational taxonomic units (OTUs)) in a sorghum diversity panel (Deng et al., 2021). However, previous attempts at linking plant genes to the abundance of specific groups of microbes have had limited success due to small population size, limited host genetic diversity, or due to insufficient taxonomic resolution (Beilsmith et al., 2019; Liu et al., 2021). It was observed previously (Zhu et al., 2016) that soil microbial communities drastically change in response to N fertilization. In bulk soil, this is likely due to a direct effect of N application or lack thereof. In rhizospheres, however, only a subset of the observed changes can be attributed to direct effects of nitrogen (N) fertilization, while particular microbial groups may be subject to

indirect effects induced by the plant host in response to N availability or deficiency (Meier et al., 2021). A possible explanation for this could be that during most of the interval between maize domestication and the present, beneficial plant-microbe interactions have evolved in low-input agricultural systems characterized by relative scarcity of nutrients, predominantly nitrogen (Brisson et al., 2019). This is in stark contrast to the modern agricultural environment that has been the norm since the 1960s, in which plants are supplied with large quantities of inorganic N fertilizer (Cao et al., 2018). As a consequence, previous selection pressure to retain traits favorable under low N conditions, including plant growth-promoting microbes, has been largely reduced in modern maize breeding programs (Haegele et al., 2013; Zhu et al., 2016). Thus, if a microbial group is indeed under host genetic control and has an effect on plant fitness (i.e., promotes plant development or increases crop yield) under either N condition, we would expect the rhizobiome trait to be under host selection.

In the present study, we evaluate the role that selection on plant genetic factors has played in shaping the maize rhizobiome under different N conditions. We employ the maize diversity panel, a set of maize lines selected for maximum representation of genetic diversity and growth in temperate latitudes (Flint-Garcia et al., 2005). This population has previously been used to determine the heritability of leaf microbiome traits and to perform genome-wide association studies (GWAS) on a number of different phenotypes (Wallace et al., 2018). We collected replicated data on the rhizobiome of 230 lines drawn from this panel when grown under either high N (+N) and low N (-N) conditions in the field. For 150 microbial groups present in the rhizosphere (referred to as “rhizobiome traits”), which were abundant and consistently reproducible, we quantify the degree to which variation is subject to plant genetic control, and test for evidence of selection under either or both N conditions. Using a set of 20 million high density single nucleotide polymorphisms (SNPs), we perform GWAS for each rhizobiome trait identifying genomic loci that are associated with one or more rhizobiome traits. Through

comparison with gene expression data generated for the same population, we determine whether genes near microbe-associated plant loci are preferentially expressed in root tissue. Lastly, we evaluate whether the abundance of each microbial group in the rhizosphere is correlated with plant performance traits measured in the field, and whether microbe abundance and plant performance depend on the allele variant at selected microbe-associated plant loci. The results presented in this study lay the groundwork for future endeavors to investigate the molecular mechanisms of specific plant-microbe interactions under agronomically relevant conditions.

Results

Characterization of the rhizobiome for diverse maize genotypes under two different N conditions

Paired-end 16S sequencing of 3,313 rhizosphere samples from 230 replicated genotypes of the maize diversity panel (Flint-Garcia et al., 2005) were collected from field experiments conducted under both +N and -N conditions (**Materials and Methods**). At the time of sampling, visible phenotypic differences were observable between +N and -N plots as measured through aerial imaging (details are reported in Rodene et al., 2022 using the same experimental field). Sequencing produced 216,681,749 raw sequence reads representing 496,738 unique amplicon sequence variants (ASVs) (**Materials and Methods**). Raw reads were subjected to a series of quality checks and abundance filters following a workflow for 16S sequencing data analysis by (Callahan et al., 2016a), which resulted in a curated dataset of 3,626 ASVs for 3,306 samples, and 105,745,986 total ASV counts (**Supplementary File 1**). This dataset includes ASVs that are highly abundant across the maize diversity panel and reproducible in both years of sampling. Constrained Principal Coordinates analysis calculated from the abundances of 3,626 ASVs shows divergence of samples collected under either -N or +N treatment (**Figure 1A**),

148 which indicates that the microbiomes differ between these two experimental conditions
149 (PERMANOVA p-value for N treatment < 0.001).
150
151 An initial analysis looking at high-level rhizobiome traits (Principal Components and alpha
152 diversity metrics derived from the ASV table) shows the same pattern of divergent microbial
153 communities between N treatments, and in particular under the -N treatment there is evidence
154 for the association of plant genomic loci and microbiome composition (**Figure 1 – figure**
155 **supplement 1**). To study changes in rhizobiome composition more accurately, the final 3,626
156 ASVs were clustered into n = 150 distinct microbial groups ("rhizobiome traits"), spanning 19
157 major classes of rhizosphere microbiota (**Figure 1B, Supplementary Files 2 & 3**) using a
158 method previously described (Meier et al., 2021, **Supplementary Methods**). Of these
159 rhizobiome traits, 79/150 (52.7%) groups were significantly more abundant in samples collected
160 from the +N condition (t-test, $p < 0.05$), 53/150 (35.3%) significantly more abundant in samples
161 collected from the -N condition, and 18/150 (12.0%) showed no significant difference in
162 abundance between the two treatments. In several cases, more closely related microbial groups
163 exhibit shared patterns of differential abundance between N treatments (**Figure 1 – figure**
164 **supplement 2A**).
165
166 **Rhizobiome traits are more heritable under -N conditions**
167 The abundance of each of the 150 rhizobiome traits was assessed separately for +N and -N
168 conditions, and the heritability (proportion of total variance explicable by genetic factors) was
169 estimated using an approach following a previous study (Deng et al., 2021) (**Materials and**
170 **Methods)**. Rhizobiome traits were comparatively more heritable under -N than +N conditions
171 (paired Student's t-test, $p = 0.021$, **Figure 1C**). We found 34/150 (22.7%) microbial groups to be
172 significantly heritable (permutation test, $p < 0.05$, **Materials and Methods**) under both N
173 conditions, 18/150 (12%) only under +N conditions, and 27/150 (18%) only under -N conditions.

Twelve rhizobiome traits exhibited estimated $h^2 > 0.6$ in both +N and -N conditions (**Figure 1 – figure supplement 3**). These include 4 groups of ASVs assigned to the order *Burkholderiales* (the genus *Pseudoduganella*, an unknown genus in the *Comamonadaceae* family, the family *A21b*, and *Burkholderia oklahomensis*) and 2 groups in the *Sphingomonadales* order (*Sphingobium herbicidovorans 1* and an unknown genus in the *Sphingomonadaceae* family). Notably, closely related microbial groups did not exhibit obvious patterns of shared high or low estimated heritabilities (**Figure 1B**). As heritabilities and responses to treatments can vary considerably within families, genera, and lower taxonomic ranks, this underscores the importance of adequate taxonomic resolution when analyzing rhizosphere microbial communities. We further observed that more abundant microbes in the rhizosphere also tend to be more heritable. The correlation of relative abundance vs. heritability was $r = 0.29$ (Pearson's correlation test, $p = 3.4 \times 10^{-4}$) for +N and $r = 0.39$ (Pearson's correlation test, $p = 1.1 \times 10^{-6}$) for -N (**Figure 1 – figure supplement 2B**).

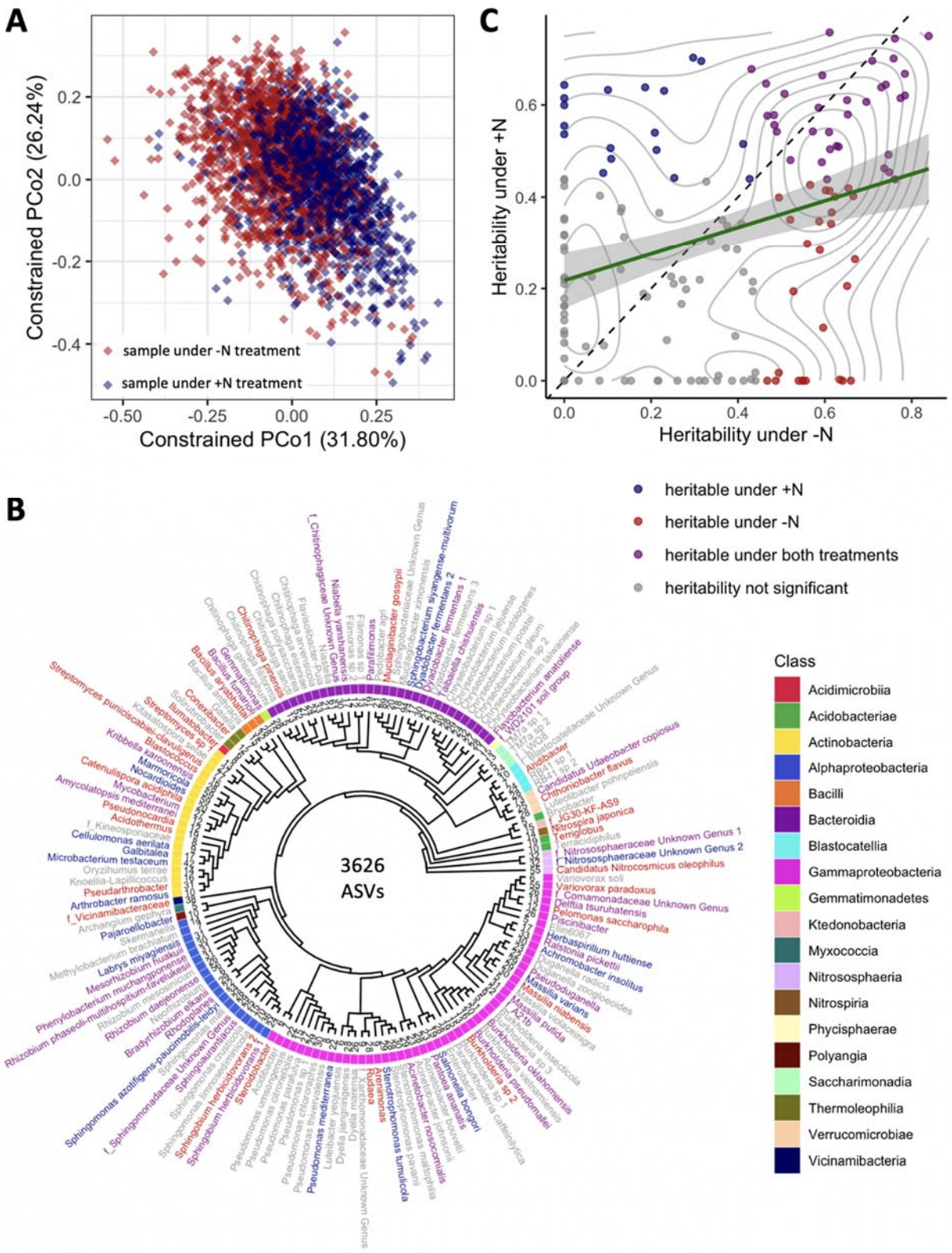
A
Constrained PCo2 (26.24%)
Constrained PCo1 (31.80%)
sample under -N treatment
sample under +N treatment
C
Heritability under +N
Heritability under -N
B
heritable under +N
heritable under -N
heritable under both treatments
heritability not significant
3626
ASVs
Class
Acidimicrobiia
Acidobacteriae
Actinobacteria
Alphaproteobacteria
Bacilli
Bacteroidia
Blastocatellia
Gammaproteobacteria
Gemmatimonadetes
Ktedonobacteria
Myxococcia
Nitrososphaeria
Nitrospiria
Phycisphaerae
Polyangia
Saccharimonadia
Thermoleophilia
Verrucomicrobiae
Vicinamibacteria

Figure 1: Diversity, phylogenetics, and heritability of rhizobiome traits. (**A**) Constrained ordination analysis showing the largest two principal coordinates calculated from the abundances of 3,626 ASVs. Each diamond represents one sample collected from plants under +N (blue) and -N (red) treatment, respectively. Note the separation of N treatments along PCo1. (**B**) Phylogenetic tree of 150 taxonomic groups of rhizosphere microbiota ("rhizobiome traits") generated by clustering 3,626 ASVs. Families are prefixed with "f_", genus and species names are given where known. Numbers at tree tips indicate distinct ASVs in each group. Label colors indicate heritability of each rhizobiome trait as in panel C. (**C)** Heritability (h^2) calculated for all 150 rhizobiome traits under +N and -N treatments. Green line indicates linear regression with 95% confidence interval, $r^2 = 0.104$. Diagonal dashed line denotes identity. Grey lines mark density of data points. Colors indicate whether traits are significantly heritable under either or both N treatments, as determined through a permutation analysis using 1000 permutations.

Figure 1 – figure supplement 1: GWAS of high-level rhizobiome traits:

(A, B) The first 10 principal components were calculated for both the high N (left) and low N (right) treatment using the best linear unbiased prediction (BLUPs) of the log(relative abundance) of 3618 ASVs in 230 maize genotypes. Total variance explained was 60.8% for +N and 65.3% for -N.

(C) The largest contributors to PC1 differed between the two experimental conditions. Microbial groups that account for at least 1% of total variance are annotated in the pie charts.

(D, E). Notable GWAS signals above the significance threshold (dashed red line) were observed in the -N treatment for PC1 and the InvSimpson diversity metric (red arrows), indicating genomic loci that affect high-level metrics of the rhizobiome. The other PCs and diversity metrics had no strong GWAS signals and were not shown.

Figure 1 – figure supplement 2: Abundance and heritability of 150 microbial groups.

(A) Phylogenetic tree of 150 microbial groups. Colors indicate differential abundance between the +N and -N treatment.

(B) The mean abundance (mean BLUP of log(relative abundance) across 230 maize genotypes) of each microbial group was plotted against the heritability score in the +N and -N treatment. A positive correlation is observed in both environments, indicating that more abundant microbes in the rhizosphere also tend to be more heritable.

Figure 1 – figure supplement 3: Annotations of heritable microbial groups. (A) The 12 most heritable microbial groups with heritability > 0.6 (drawn lines) under both N conditions were annotated by name. (B) Taxonomy of the 12 most heritable groups.

Rhizobiome traits are related with plant fitness and predominantly under purifying selection

Under the hypothesis that the rhizobiome traits have effects on plant fitness, we sought to estimate the selection gradients under different N treatments (Lande and Arnold 1983). To reduce biases due to environmental covariances (Rausher 1992), the standardized BLUP values of the microbial traits were fitted into the fitness function (See **Materials and Methods**). For the selection gradient estimation, the canopy coverage (CC) obtained from UAV imaging was used as a proxy for plant fitness. As a result, we identified 58 unique rhizobiome traits exhibiting significant linear selection gradients (bootstrapping p-value < 0.05) under +N (28 traits) and -N (46 traits) treatments (**Figure 2 – figure supplement 1**). Additionally, 4 rhizobiome traits showed significant quadratic selection gradients (+N: *Luteolibacter pohnpeiensis* (-2.627913e-05, p-value = 0.044), -N: *Blastococcus* (8.516159e-06, p-value = 0.03), *Pseusomonas umsongensis* (-2.003792e-05, p-value = 0.04), *Chthoniobacter flavus* (-5.807404e-05, p-value = 0.028)).

Selection acting on rhizobiome traits can happen either by purging deleterious alleles (purifying selection) or by elevating the frequencies of advantageous alleles (positive selection). To evaluate the mode of selection at the genomic level, a Bayesian-based method (Genome-wide Complex Trait Bayesian analysis, or GCTB) was used to test for each rhizobiome trait (**Materials and Methods**). A set of n = 834,975 independent SNPs was used to estimate their effects on 150 rhizobiome traits as well as 17 conventional plant traits collected from the same population in the same field experiments (**Materials and Methods, Supplementary File 4**). Using the relationship between effects of non-zero SNPs and their minor allele frequencies (MAFs) as a proxy for the signature of selection (Zeng et al., 2018), the S parameter was jointly estimated from the GCTB analysis for rhizobiome traits and plant traits. According to Zeng (Zeng et al., 2018), if S = 0 (i.e., the posterior distribution of S is insignificantly different from zero), the SNP effect is independent of MAF, suggesting a neutral selection. If there is selection acting on the trait, the SNP effect can be positively (S > 0) or negatively (S < 0) related to MAF, indicating positive and purifying selection, respectively.

We report 10 rhizobiome traits that showed both significant linear selection gradients and significant S parameters (**Figure 2A**). Under these stringent criteria, 9 rhizobiome traits show evidence of purifying selection under +N or under -N. One microbial group (*Bacillus fumarioli*) showed positive S values indicating that this trait might have been a target of positive selection. Relative to rhizobiome traits, plant leaf traits and nutrient traits were both more likely to exhibit evidence of selection within this maize population. Three out of 15 plant leaf traits, i.e., leaf area (LA), leaf fresh weight (FW), and leaf dry weight (DW) (**Materials and Methods**), exhibited S > 0 values under the +N condition, consistent with positive selection, while only one of the three exhibited a slightly negative S value in the -N condition and in that case exhibited a pattern consistent with weak purifying selection (**Figure 2B)**. Note that the three leaf-related traits are not independent. The pairwise correlation coefficients are 0.92, 0.91, and 0.94, for LA and FW,

LA and DW, FW and DW, respectively. Of the 11 micronutrient traits evaluated, 9/11 and 4/11 showed significantly negative S values in trait data collected under +N and -N conditions, respectively. From the same GCTB analysis, estimates of the number of SNPs with non-zero effects were substantially lower for rhizobiome traits than for conventional plant traits, whereas the differences were insignificant between the two N treatments for both rhizobiome and plant traits (**Figure 2C**). Using these non-zero effect SNPs, we plotted their minor allele frequency vs. the minor allele effect. As expected, in the case of positive selection (*Bacillus fumarioli*), we observed a skew towards higher MAF and in the case of purifying selection (*f_Comamonadaceae Unknown Genus*), a skew towards lower MAF (**Figure 2D)**.

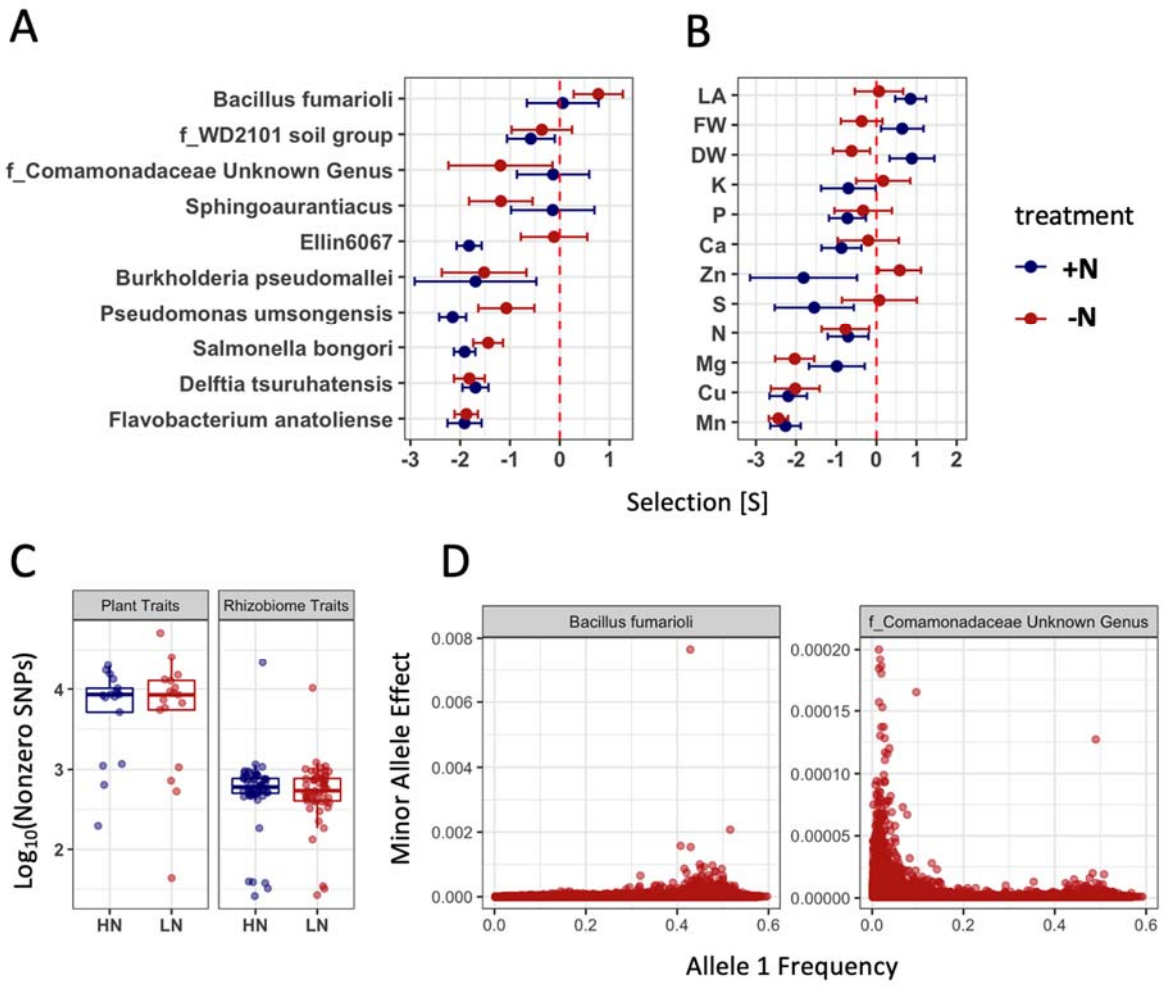

Figure 2: Population parameters estimated from genome-wide SNPs for plant and rhizobiome traits. Selection coefficients (S value) of rhizobiome (**A**) and plant (**B**) traits calculated for both N treatments using genome-wide independent SNPs. A negative S value indicates negative (purifying) selection, and a positive S value indicates positive (directional) selection. Traits are shown that show significant selection under one or both N treatments. (**C**) Number of SNPs showing non-zero effects for both plant and rhizobiome traits. (**D**) Examples of positive (*Bacillus fumarioli*) and purifying selection (*f_Comamonadaceae Unknown Genus*) showing minor allele effect vs. allele 1 frequency with data skew to the right and to the left, respectively.

Figure 2 – figure supplement 1: Rhizobiome traits exhibit significant linear selection gradients (bootstrapping p-value < 0.05) under +N and -N treatments

Genes underlying microbe-associated plant loci are preferentially expressed in root tissue

The observation that many rhizobiome traits are both under significant host genetic control and targets of selection suggests it may be possible to detect individual large effect loci controlling rhizobiome traits. To investigate this, we performed GWAS using each of the 150 rhizobiome traits. This analysis was done separately for the -N and +N conditions, as N deficiency induces dramatic changes in plant metabolism, including changes in root gene expression (Singh et al., 2022) and root exudation (Zhu et al., 2016), and because N applied to the field directly impacts soil and rhizosphere microbiomes (Meier et al., 2021). We focused on “hotspots” along the genome where we find the highest cumulative density of significant associations between SNPs and any rhizobiome traits under either N treatment, because morphological (i.e., root architecture) or physiological (root exudation) changes may simultaneously affect several rhizobiome traits. For this purpose, we split the maize genome into 10 kb genomic windows and

tallied the number of significant ($p < 10^{-7.2}$) GWAS signals in each window. This analysis revealed 622 genomic regions containing at least one significant GWAS signal, and we refer to these regions as microbe-associated plant loci (MAPLs) (**Materials and Methods**). We report these MAPLs alongside nearby genes in **Supplementary File 5.** 104 out of 150 microbial groups were associated with at least one of the 622 loci.

To reduce false discoveries, we decided to discuss a subset of 119 MAPLs here, that had at least two significant GWAS signals. Among these 119 MAPLs, 69 were observed under +N treatment and 50 under -N treatment (**Figure 3A, Supplementary File 5**). Of the 150 rhizobiome traits evaluated here, 35 were associated with at least one of the 119 MAPLs, with 21 rhizobiome traits associated with 69 MAPLs under the +N treatment and 17 rhizobiome traits with 50 MAPLs under the -N treatment. 3 rhizobiome traits (*f_Chitinophagaceae Unknown Genus*, *Sphingoaurantiacus*, and *f_Vicinamibacteraceae*) showed significant associations under both N treatments, albeit with different plant loci. No loci were found that had associations with rhizobiome traits under both N treatments, which is expected as GWAS analyses were done separately for different N treatments and the microbial groups studied here were partly distinguished based on differential abundance in response to N treatments.

We hypothesized that many plant genes underlying MAPL hotspots may exert control over the rhizosphere microbiome via changes in root physiology, architecture, and exudate composition (Vandenkoornhuyse et al., 2015) and may therefore be preferentially expressed in root tissue. Transcribed sequences of 97 gene models were completely contained within ±10 kb of the 119 MAPL hotspots identified here, where 114/119 MAPLs contained between 1 and 5 genes. We evaluated the expression of these MAPL genes relative to the overall patterns exhibited by all genes outside the MAPL regions in seven tissues using published expression data from the same maize population (Kremling et al., 2018). Expression data was available in this dataset for

73 out of 97 MAPL genes across 298 maize genotypes from tissue samples collected at germination and during flowering time. These MAPL genes, when compared to (n = 29,771) other genes available in the dataset, show on average significantly higher expression in the germinating root, the germinating shoot, and the third leaf base (**Figure 3B**).

To complement the gene expression data provided by Kremling et. al, we selected 4 diverse and well characterized maize genotypes (K55, W153R, B73, and SD40). Plants were grown in a controlled greenhouse environment under standard N and N deficient conditions and gene expression was analyzed in roots and shoots of two-week old seedlings (for details refer to Xu et al, 2022). In agreement with the dataset provided by Kremling et al, significantly higher expression of 97 MAPL genes was observed in root but not leaf tissue compared to (n = 44,049) other genes available in this dataset (**Figure 3C**). No strong physiological response to N deficiency was expected for 2-week-old seedlings and no significant differences were observed in the pattern of MAPL gene expression between the two N treatments.

Collectively, these data are consistent with the hypothesis that rhizobiomes are at least in part genetically controlled by the host plant in a process mediated by plant gene expression.

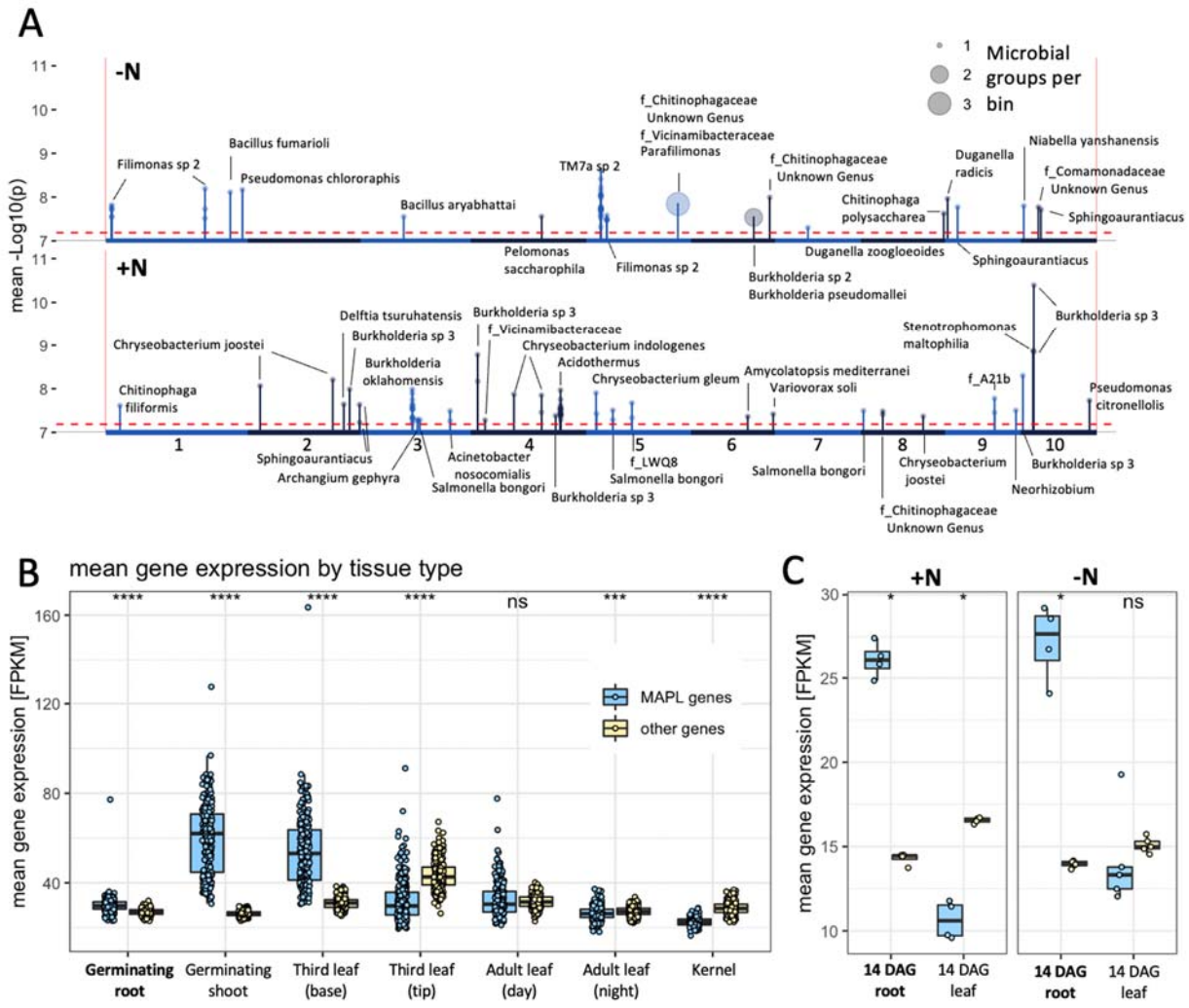

Figure 3: **Microbe associated plant loci (MAPLs) contain genes expressed in roots.** (**A)** GWAS of 150 rhizobiome traits reveals microbe-associated plant loci across the maize genome. Dashed line indicates the -log10(p) = 7.2 significance level for GWAS signals. Circles on top of peaks at each MAPL indicate the number of rhizobiome traits associated with each locus. Each MAPL is annotated with the associated rhizobiome trait(s) that showed significant GWAS signals. (**B**) Mean gene expression of 73 MAPL genes and 29,771 other genes in seven tissue types, measured in 298 genotypes of the maize diversity panel (Kremling et al., 2018). (**C**) Mean gene expression of 97 MAPL genes and 44,049 other genes in two tissue types, measured in the present study in four maize genotypes under +N and -N treatments.

Heritable and adaptively selected rhizobiota are associated with plant phenotypes

We investigated the correlation of microbe abundance with 17 plant traits, including leaf physiology, leaf micronutrient traits, and traits extracted from aerial images (**Materials and Methods**) to identify potential plant phenotypic consequences of variation in the abundance of specific rhizosphere microbes. Several rhizobiome traits were significantly correlated ($p < 0.01$) with measures of plant performance, such as leaf area, leaf dry weight and fresh weight, and with several measures of leaf micronutrients such as nitrogen, sulfur, and phosphorus (**Figure 4 – figure supplement 1**). The trait that was most strongly linked to microbe abundance was leaf canopy coverage (CC). In total, 62 microbial groups – more than expected by chance (permutation test, $p < 0.001$) – were significantly (Pearson correlation test, $p < 0.01$) associated with CC (marked in **Figure 4** in green for positive correlation and in red for negative correlation). 30 microbial groups under +N and 35 under -N were positively correlated with CC. 14 groups under +N and 12 under -N were negatively correlated with CC. 15 microbial groups were associated with CC under +N treatment, 18 under -N treatment, and 29 showed a significant association under both N treatments (**Figure 4A**). Under both N treatments, we observe an association between heritability and the correlation with CC, which was statistically significant (Pearson correlation coefficient $r = 0.39$, $p = 4 \times 10^{-6}$) for +N and even more significant ($r = 0.49$, $p = 1.7 \times 10^{-9}$) under the -N condition (**Figure 4B**).

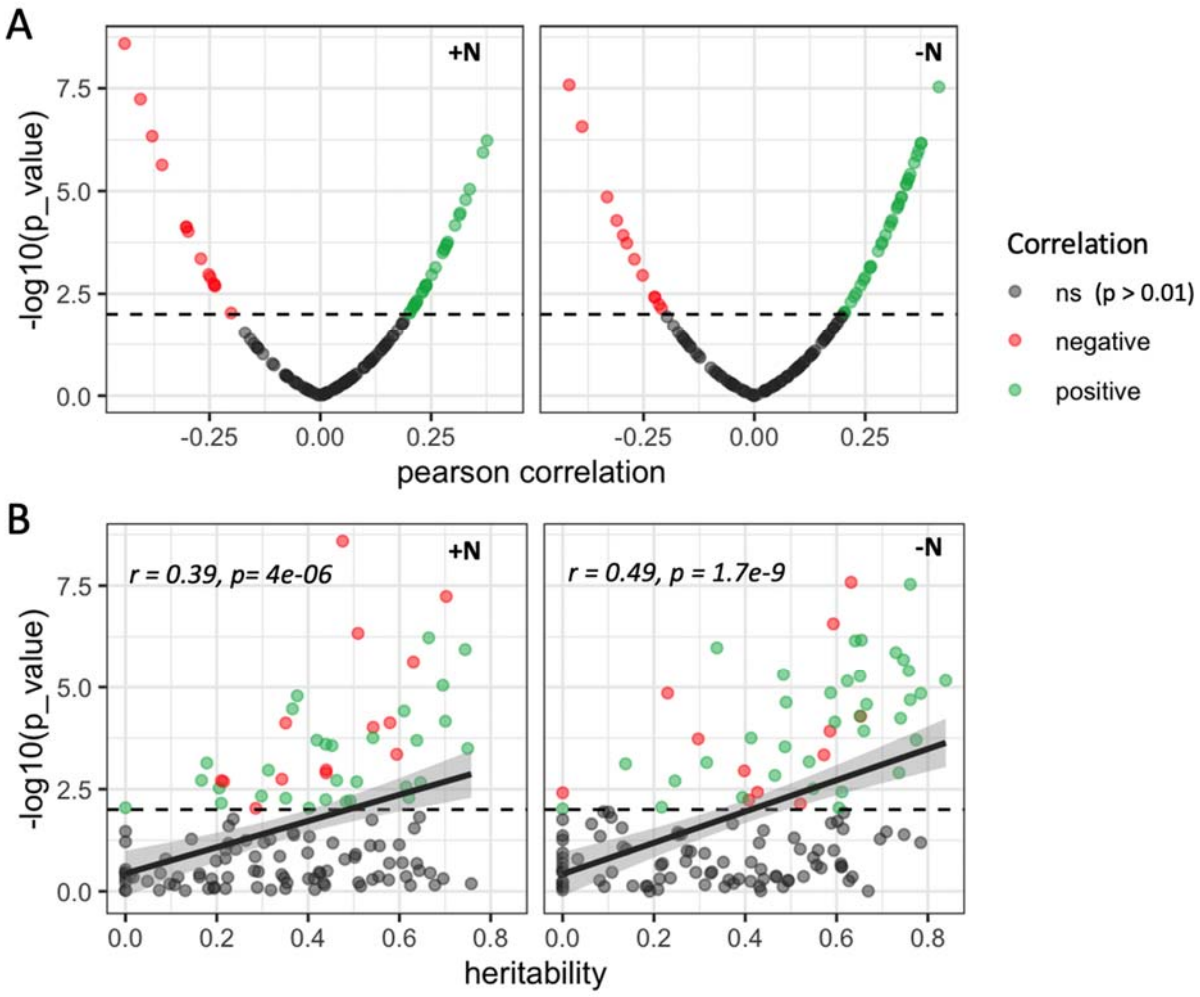

Figure 4: Heritable microbial groups tend to be correlated with whole plant canopy coverage. (**A**) Distribution of statistical significance and correlation values for the relationship between canopy coverage (CC) and each of 150 microbial groups under either +N or -N conditions. Dashed line indicates significance level (p = 0.01). (**B**) Relationship between the estimated heritability of individual rhizobiome traits and correlation of the same individual rhizobiome traits with variation in CC. Dashed line indicates significance level (p = 0.01).

Figure 4 - figure supplement 1: Correlation of microbe abundance with 17 agronomic and micronutrient traits under +N (blue) and -N (red) conditions. Each dot represents one of 150

rhizobiome traits. X axis shows correlation with agronomic trait (r value), y axis shows significance, dashed line shows p=0.01 level of significance. CC_Aug12, EXG_Aug12: canopy coverage and excess green index measured on Aug. 12, 2019; CHL: chlorophyll content, DW: dry weight, FW: fresh weight, LA: leaf area.

Figure 4 - figure supplement 2: Microbial traits that correlate with canopy coverage.
Venn diagram shows a total 62 microbial traits that correlate with canopy coverage either under +N, -N or both treatments. For the 62 listed rhizobiome traits, colored dots summarize various statistics that indicate association with the host plant genetics and performance.

We summarize the relationship of the analyses conducted in this study under either N treatment for the 62 microbial groups that are correlated with CC. 44/62 (71%) are heritable and 13/62 (21%) are under selection under either or both N treatments (**Figure 4 – figure supplement 2)**. 56/62 (90%) show strong GWAS signals in 174/467 (39%) of the MAPLs identified here, which contain 255/395 (65%) of possibly microbe-associated genes. Two microbial groups, *f_Comamonadaceae* Unknown Genus and *Sphingoaurantiacus*, are of particular interest as they overlap in all performed assays, showing evidence of heritability and selection, a strong GWAS signal in associated plant genomic loci positive correlation with canopy coverage. The complete summary data for all 150 microbial groups are available in **Supplementary File 3**.

Overall, our data show a clear trend that the 62 microbial groups associated with plant performance also tend to be associated with host genetics, and the datasets provided here can be used to design more targeted experiments to confirm associations of rhizosphere microbial groups with plant genetics and performance on a case-by-case basis.

Allelic differences at microbe-associated plant loci predict microbe abundance

We identified several strong GWAS signals that link plant genomic loci to rhizobiome traits (**Figure 3A**). Such signals indicate that the pattern of SNPs at a given locus (i.e., the genetic architecture) has a large magnitude of effect attached to the abundance of the associated microbial groups. Next, we sought to determine whether a particular allele (either the major or the minor variant) in our maize population is associated with an increased or decreased abundance of the corresponding microbe.

The unknown genus in the *Comamonadaceae* family mentioned above, while unnamed and uncharacterized, shows high heritability under both N treatments (h^2 = 0.610 under +N, and 0.651 under -N, **Figure 1B & 1C**), and shows evidence of being under purifying selection under -N (**Figure 2A & 2D**). Under the same environmental conditions, a significant MAPL controlling variation in microbial abundance is detectable on maize chromosome 10 (**Figure 3A** and **Figure 5A**). This same rhizobiome trait is among those that are positively correlated with CC under both -N ($r = 0.347$, $p = 5.313 \times 10^{-6}$) and +N ($r = 0.314$, $p = 3.845 \times 10^{-5}$) (**Figure 4A**). A total of five annotated gene models are located near the peak of significant SNP markers that define the chromosome 10 MAPL for this rhizobiome trait (**Figure 5A & 5B**). A linkage disequilibrium block was observed between 23.90 and 23.96 MB on maize chromosome 10, spanning the set of significantly associated SNPs and three candidate genes Zm00001d023838, Zm00001d023839 and Zm00001d023840 (**Figure 5C**). In accordance with **Figure 3C**, these genes are preferentially expressed in roots (**Figure 5 – figure supplement 1**). As described above, the abundance of the *f_Comamonadaceae* genus was significantly correlated with variation in CC, shown here for the -N treatment (**Figure 5D**). Next, we used the haplotype information at the target SNP to mark genotypes that carry the major allele or the minor allele, respectively, and the abundance of the *f_Comamonadaceae* genus was significantly higher in rhizosphere

samples collected from maize genotypes carrying the major allele than in samples collected from maize genotypes carrying the minor allele (**Figure 5E)**. However, CC was not significantly different between maize genotypes carrying either the major or minor allele of the chromosome 10 MAPL (**Figure 5F**).

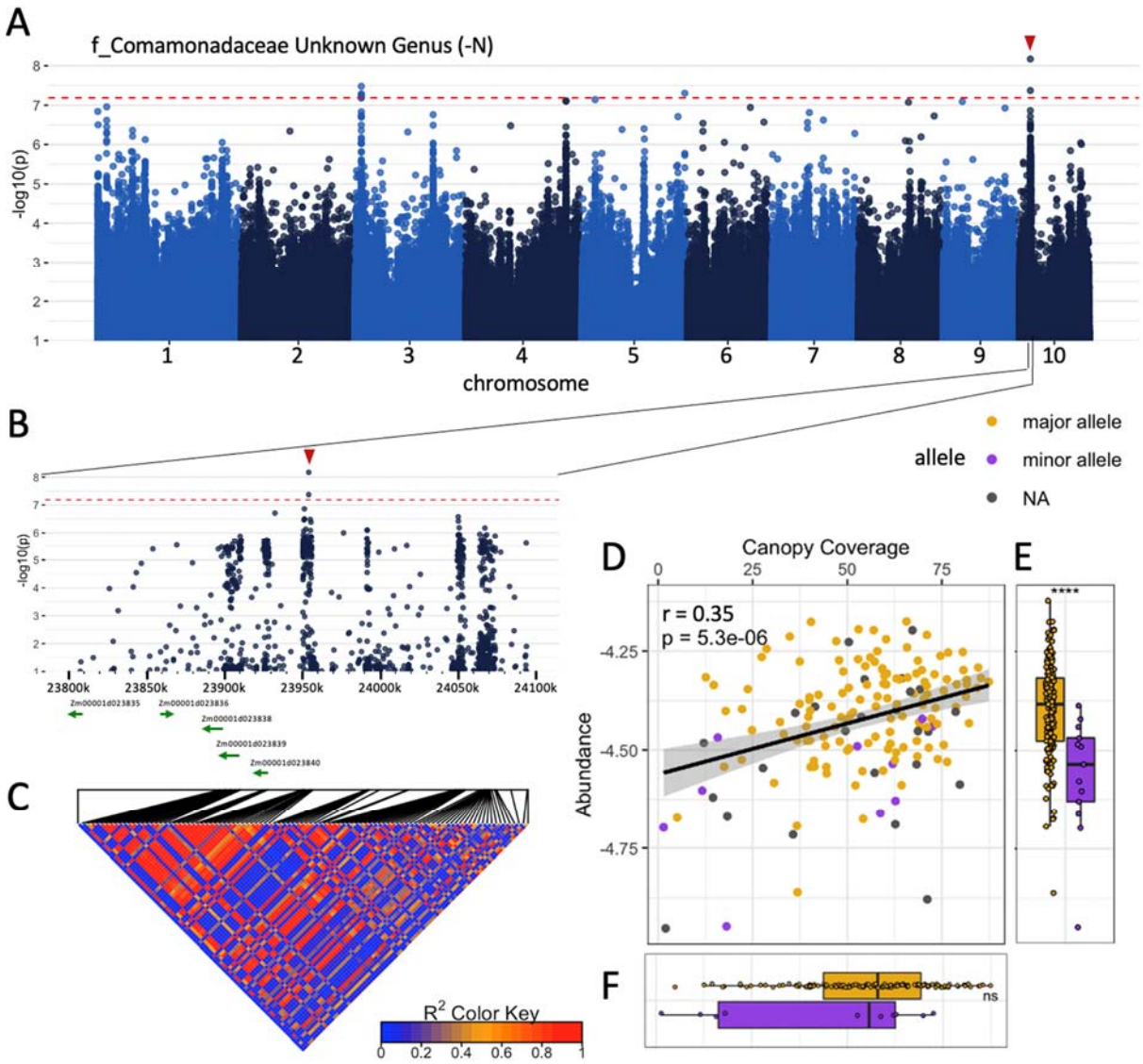

Figure 5: Abundance of heritable, adaptively selected microbes depends on allelic differences at MAPLs. (**A**) Results of a genome wide association study conducted using values for the rhizobiome

trait (*f_Comamonadaceae Unknown Genus*) observed for ~230 maize lines grown under nitrogen deficient conditions. Alternating colors differentiate the 10 chromosomes of maize. Dashed line indicates a statistical significance cutoff of -log10(p) = 7.2. (**B**) Zoomed in visualization of the region containing the peak observed on chromosome 10. (**C**) Linkage disequilibrium among SNP markers genotyped within this region, calculated using genotype data from 271 lines (**D**) Correlation plot of microbe abundance vs. canopy coverage (CC). Each point represents a maize genotype. Differences in microbe abundance (**E**) and CC (**F**) are marked between genotypes carrying the major allele (gold) vs the minor allele (purple) at the target SNP (red arrow in panel A and B).

Figure 5 – figure supplement 1: Genes at MAPL are preferentially expressed in roots.
Gene expression in leaf tissue vs roots of three genes at chr 10 locus in main text **Figure 5**. Maize genotypes are the same as in main text **Figure 3C**. Genes Zm00001d023838 and Zm00001d023839 show significantly higher expression in roots.

The example discussed here shows a three-way association of the abundance of a particular microbial group in the rhizosphere, a corresponding locus on the maize genome, and plant performance in the field. The datasets provided alongside this publication contain several such associations and may serve as the basis for more targeted experiments to establish a direction of causation between microbe abundance and plant performance, and to shed light on the genetic mechanisms that shape symbiotic relationships between the plant host and associated rhizosphere microbes.

Discussion

This study profiled the rhizosphere inhabiting microbiota of several hundred maize genotypes under agronomically relevant field conditions. Through a 16S rDNA-sequencing based approach, we identified a set of 150 reproducible rhizobiome traits based on 3,626 ASVs that were highly abundant and consistently reproducible in this maize diversity panel. The phylogenetic tree in **Figure 1B** may deviate from the consensus microbial phylogeny since only the 350bp ribosomal V4 region was used to establish the relationship between groups, and more accurate phylogenetic clustering should be considered in future studies with emphasis on the evolution of plant-microbe associations. In total, 79 out of the 150 rhizobiome traits (52%) showed significant evidence of being influenced by host plant genotype in one or more environmental conditions. The estimated heritability of rhizobiome traits in this study ranged from 0 to 0.757 for the +N treatment (mean 0.320) and from 0 to 0.839 for the -N treatment (mean 0.352). A comparable study of the rhizobiomes in a sorghum diversity panel estimated similar values (Deng et al., 2021). A previous study on the same maize diversity panel (Wallace et al., 2018) investigated the heritability of 185 individual OTUs and 196 higher taxonomic units measured in the leaf microbiome. The study reported only 2 OTUs and 3 higher taxonomic groups showing significant heritability using the same permutation test we employed in this study. This may indicate that plant genetics have a stronger influence on rhizosphere colonizing microbes than on leaf colonizing microbes. One reason for this may be that there is a direct pathway for plant-to-microbe communication via root exudates (Doornbos et al., 2012). In contrast, no equivalent exchange of chemical information has been reported above ground, with the possible exception of aerial root mucilage (Van Deynze et al., 2018).

We observed relatively higher heritability for rhizobiome traits quantified from plants grown in the -N treatment than under the +N treatment. This outcome is consistent with a model where

394 the partnerships between microbiomes and plants were established in natural and early
395 agricultural systems which were predominantly N limited (Brisson et al., 2019). N insufficiency in
396 maize induces dramatic changes in physiology (Ciampitti et al., 2013), gene expression (Chen
397 et al., 2011; Singh et al., 2022), root architecture (Gaudin et al., 2011) and root exudation
398 (Baudoin et al., 2003; Haase et al., 2007; Zhu et al., 2016). Consistent with this, N fertilization or
399 the lack thereof has substantial consequences on plant-microbe associations. In this study, 12%
400 of rhizobiome traits were only significantly heritable under the +N treatment, and 18% only
401 under the -N condition, and GWAS revealed plant-microbe associations at different genomic loci
402 depending on the N treatment. Previous observations have also reported that rhizosphere
403 microbial communities are highly sensitive to environmental conditions, in particular to N
404 deficiency (Meier et al., 2021; Zhu et al., 2016). This finding emphasizes the need to optimize
405 microbial communities not only for a specific host but also for specific levels of N fertilization.
406
407 Our results suggest that the capacity of maize plants to encourage or discourage colonization of
408 the rhizosphere by specific microbiota has been a target of selection. The BayesS method
409 leverages the relationship between the variance of SNP effects and MAF as a proxy of
410 natural selection in the distant past. This method detects signatures of natural selection on
411 SNPs associated with microbiome traits but is not directly indicative of selection acting on
412 the particular microbes. Indeed, we observed purifying selection acting on genetic variants
413 associated with the abundance of 9 rhizosphere traits, 7 in the +N and 7 -N environment,
414 respectively. Several rhizosphere denizens whose abundance showed evidence of being a
415 target of purifying selection in the host genome have been linked to plant growth promoting
416 activities, most notably *Pseudomonas* (Otieno et al., 2015; Preston, 2004) and *Burkholderia*
417 (Bernabeu et al., 2015; Kurepin et al., 2015). *Bacillus fumarioli,* which showed evidence of
418 positive selection, has previously been observed in plant rhizospheres, particularly in maize

(Garbeva et al., 2008), and several strains of *Bacillus* plant growth promoting activities (Kumar et al., 2012). Notably, not all traits that are heritable are expected to be under selection, as traits can be heritable, i.e., transmitted from one generation to the next, without impacting the fitness or performance of offspring individuals under the conditions under which recent natural and/or artificial selection has occurred. To further approve the beneficial effects of the microbes on the plant fitness, additional functional analyses (i.e., inoculation experiments) are warranted, and that naturally occurring microbe-plant symbiosis may be harnessed for further crop improvement.

Among the 150 rhizobiome traits analyzed here, 62 showed a significant correlation with measurements of canopy coverage collected from the same field experiment. In particular, the observed link between heritability of microbes and correlation with plant performance may indicate a symbiotic relationship of the host plant and root-associated microbes. However, while our data show correlations between microbe abundance and plant phenotypes, further experiments are required to determine the direction of causation and investigate potential mechanisms by which microbe abundance could influence phenotypic changes in the host. We observe that the majority of rhizobiome traits that are correlated with canopy coverage are both heritable and associated with one or more microbe-associated plant loci (MAPLs), and genes linked to variation in rhizobiome traits via GWAS were highly expressed in roots across genotypes in multiple independent gene expression datasets. This suggests a number of potential mechanisms for host plant genotypes to influence the composition of the rhizobiome. For example, two of the three genes associated with the MAPL highlighted in Figure 5 (Zm0001d023838 and Zm0001d023839) are preferentially expressed in roots (**Figure 5 – figure supplement 1**). According to MaizeGDB, both are protein coding genes that have not yet been characterized in maize. Known Zm0001d023838 orthologs in Arabidopsis encode AUXILIN-

LIKE1 and AUXILIN-LIKE2, and overexpression of auxilin-like proteins in Arabidopsis has been shown to inhibit endocytosis in root hair cells (Ezaki et al., 2006). Overexpression of auxilin-like proteins has also been shown to confer resistance to root-borne bacterial pathogens in rice (Park et al., 2017). This indicates a possible link between root hair physiology and an altered microbiome. Although substantial further experimentation and study remains necessary, adjusting the expression of particular MAPL genes identified here may be an avenue to directly influence and engineer the abundance of targeted microbial groups in the rhizosphere to the benefit of the plant.

We evaluated associations between rhizobiome traits and a number of whole plant phenotypes. The maize diversity panel has been and continues to be utilized in field experiments to determine the genetic basis of many phenotypes across diverse environments. The datasets generated here link the abundance of 150 microbial groups in the rhizosphere to genetic variation in 230 genotypes across two N treatments. Combining these public datasets with plant phenotypes collected from the same genotypes in additional environments may lead to the identification of other cases where MAPLs are associated with variation in plant phenotypes or plant performance. The results presented in this study add to an increasing body of evidence that microbial communities are actively and dynamically shaped by host plant genetic variation and may serve as the foundation for future research into particular plant-microbe relationships that may be harnessed to sustainably increase crop productivity and resilience to abiotic stress.

Materials and Methods

Field and experimental design

In this study, 230 maize (*Zea mays* subsp. *mays*) lines from the maize diversity panel (Flint-Garcia et al., 2005) were planted in May of 2018 and 2019 in a rain-fed experimental field site at the University of Nebraska-Lincoln's Havelock Farm (N 40.853, W 96.611). In both years, the experiment followed commercial maize. Individual entries consisted of 2 row, 5.3 m long plots with 0.75 m alleyways between sequential plots, 75 cm spacing between rows, and 15 cm spacing between sequential plants. In each year, the experimental field was divided into 4 quadrants and the complete set of genotypes was planted in each quadrant following an incomplete block design (**Supplementary Methods**, **Figure 6**). N fertilizer (urea) was applied at the rate of 168 kg/ha to two diagonally opposed quadrants before planting, while two quadrants were left unfertilized (-N treatment).

Rhizobiome sample preparation and sequencing

In 2018, n = 304 rhizosphere samples were collected from 28 maize genotypes (2 samples per subplot, 2 replicated plots per genotype and N treatment); and in 2019, n = 3,009 samples were collected from 230 genotypes (3 samples per subplot, 2 replicated plots per genotype and N treatment), listed in **Supplementary File 1**. Eight weeks after planting (2018: July 10 and 11; 2019: July 30, 31 and August 1), plant roots were dug up to a depth of 30 cm and rootstocks were manually shaken to remove and discard loosely adherent bulk soil. For each plant, all roots thus exposed were cut into 5 cm pieces and homogenized, and 20-30 ml randomly selected root material (with adherent rhizosphere soil) was collected to generate the rhizosphere samples (**Supplementary Methods**). DNA was isolated using the MagAttract PowerSoil DNA KF Kit (Qiagen, Hilden, Germany) and the KingFisher Flex Purification System

(Thermo Fisher, Waltham, MA, USA). DNA sequencing was performed using the Illumina MiSeq platform at the University of Minnesota Genomics Center (Minneapolis, MN, USA). In brief, 2x350 bp stretches of 16S rDNA spanning the V4 region were amplified using V4_515F_Nextera and V4_806R_Nextera primers, and the sequencing library was prepared as described by Gohl (Gohl et al., 2016).

Raw read processing and construction of microbiome dataset

Paired-end 16S sequencing reads from 3,313 samples were processed in R 3.5.2 using the workflow described by Callahan (Callahan et al., 2016a), which employs the package dada2 1.10.1(Callahan et al., 2016b). Taxonomy was assigned to amplicon sequence variants (ASVs) using the SILVA database version 138 (Yilmaz et al., 2014) as the reference. Raw ASV reads were subjected to a series of filters to produce a final ASV table with biologically relevant and reproducible 16S sequences (**Supplementary File 1**). For the constrained ordination (CAP) analysis performed here, the weighted Unifrac distance metric was used with model distance ~ year + genotype + nitrogen + block + sp + spb. Only ASVs that were highly abundant and repeatedly observed in both years of sampling were considered for downstream analysis. ASVs were clustered into 150 groups of rhizosphere microbes at the family, genus, and species level based on 16S sequence similarity and the response of individual ASVs to experimental factors (see supplementary methods).

Heritability estimation

Heritability (h^2) of rhizobiome traits was calculated separately for +N and -N conditions using maize genotypes in the 2019 dataset for which balanced data was available. For each of the 150 rhizobiome traits, combined ASV counts were normalized by converting to relative abundance and subsequent natural log transformation. Using these transformed values, h^2 was estimated following Deng et al. (Deng et al., 2021) for each rhizobiome trait using R package

sommer 4.1.0 (Covarrubias-Pazaran, 2016). In short, h^2 is the amount of variance explained by the genotype term ($V_{genotype}$) divided by the variance of the genotype and the error ($V_{genotype}$ + V_{error}/n), where n = 6 is the total number of samples (i.e., 2 replicates x 3 samples per replicate) used in this dataset. Heritability was tested for significance using a permutation test. For each trait the genotype labels of microbial abundance data were shuffled 1,000 times, and the distribution of heritabilities calculated from these shuffled datasets were used to assess the likelihood of observing the heritabilities calculated from the correctly labeled data under a null hypothesis of no host genetic control.

Calculation of selection gradient and estimation of genetic architecture parameters

We estimated the fitness function relating the fitness-related trait, i.e., canopy coverage collected on August 22 (see section "Phenotyping of plant traits"), to the abundance of the microbial groups with a generalized additive model (GAM). To reduce biases due to environmental covariances (Rausher, 1992), we employed the BLUP values for both the rhizobiome traits and the fitness-related trait. Then, we obtained linear and quadratic selection gradients from the fitted GAM models using an R package (Morrissey and Sakrejda, 2013). We ran a total of 300 univariate models (150 microbial groups x 2 N treatments).

For the rhizobiome traits, a Bayesian-based method (Zeng et al., 2018) was used to estimate genetic architecture parameters simultaneously, including polygenicity (i.e., proportion of SNPs with non-zero effects), SNP effects, and the relationship between SNP effect size and minor allele frequency. For the analysis, genotypic data of the maize diversity panel was obtained from the Panzea database and uplifted to the B73_refgen_v4 (Bukowski et al., 2018; Woodhouse et al., 2021). To account for SNP linkage disequilibrium (LD), a set of 834,975 independent SNPs (MAF >= 0.01) were retained by pruning SNPs in LD (window size 100 kb, step size 100 SNPs, $r^2 \geq 0.1$) using the PLINK1.9 software (Chang et al., 2015). In the analysis, the "BayesS" method was used with a chain length of 410,000 and the first 10,000 iterations as burnin.

Genome-wide association study

We chose to use the best linear unbiased prediction (BLUP) of the natural log transformed relative abundance of ASV counts as the dependent variable for the GWAS analysis. Since only a fraction of genotypes were sampled from the 2018 field experiment, only sample data collected in 2019 was used for the BLUP calculation. A BLUP value was calculated for each microbial group and each treatment using R package lme4 (Bates et al., 2015). In the analysis, the following model was fitted to the data: Y ~ (1|genotype) + (1|block) + (1|split plot) + (1|split plot block) + error, where Y represents a rhizobiome trait (ln(ASV count of a microbial group / total ASV count in sample)) (**Supplementary Methods**, **Figure 6**). GWAS was performed separately for each rhizobiome trait and for both the +N and -N treatment using GEMMA 0.98 (Zhou and Stephens, 2012) with a set of 21,714,057 SNPs (MAF >= 0.05) (Bukowski et al., 2018). In the GWAS model, the first three principal components and the kinship matrices were fitted to control for the population structure and genetic relatedness, respectively. To mitigate false discoveries of GWAS, Bonferroni corrections were applied based on the effective number of independent SNPs (or effective SNP number) (Li et al., 2012). The effective SNP number for the genetic marker set and population employed in this study was determined to be N = 769,690 independent markers as described previously (Rodene et al., 2022). Using an alpha value of 0.05, we determined a significance threshold of -log10(0.05/769,690) = 7.2.

RNA sequence analysis

Gene expression was analyzed using two independent datasets. The first dataset was obtained from Kremling (Kremling et al., 2018) and included RNA sequencing data from 7 different maize tissue types. The second RNA sequencing dataset was generated from root and leaf tissue collected 14 days after germination from both +N and -N treated pots using 4 genotypes from

the maize diversity panel. Libraries were sequenced using the Illumina Novaseq 6000 platform with 150 bp paired-end reads. Sequencing reads were mapped to the B73 reference genome (AGPv4) (Jiao et al., 2017; Schnable et al., 2009) and gene expression was quantified using Rsubread (Liao et al., 2019).

Phenotyping of plant traits

A total of 17 plant traits were measured in the 2019 field experiment. First, 15 leaf physiological traits were measured on the same days the rhizobiome samples were collected, and included leaf area (LA), chlorophyll content (CHL), dry weight (DW), fresh weight (FW), as well as concentrations of the elements B, Ca, Cu, Fe, K, Mg, Mn, N, P, S, and Zn. Measurement of the leaf traits was carried out as previously described (Ge et al., 2019). Two aerial imaging traits, canopy coverage (CC) and excess green index (ExG), were collected on August 12, 2019, 11-13 days after rhizobiome sample collection (Rodene et al., 2021).

Availability of data and materials

The sequencing data reported in this publication (3,313 samples) can be accessed via the following five Sequence Read Archive (SRA) accession numbers: PRJNA771710, PRJNA771712, PRJNA771711, PRJNA685208, PRJNA685228 (summarized under the umbrella BioProject PRJNA772177). Scripts used to analyze the data are available on GitHub (https://github.com/jyanglab/Maize_Rhizobiome_2022).

Acknowledgements

This study is supported by National Science Foundation EPSCoR Cooperative Agreement OIA-1557417. In Memory of James R. Alfano we thank him for his initiative and leadership at the

590 Center for Root and Rhizobiome Innovation (CRRI). We also thank Edgar Cahoon and the
591 CRRI team for setting up and maintaining an exemplary collaborative environment. We further
592 acknowledge Tom Clemente, Karin van Dijk, Daniel Schachtman, Ellen Marsh, Lisa Vonfeldt,
593 Alan Muthersbaugh, Jenny Stebbing and TJ McAndrew, for technical support. Lastly, we thank
594 the many scientists who assisted in collecting rhizosphere samples: Laure-Olivia Mbouang
595 Angoua, Bryce Askey, Abbas Atefi, Natalie Belz, Erin Bertone, Eledon Beyene, Alexandra
596 Bradley, Amanda Butera, Christian Butera, Madelyn Calvert, Noah Carroll, Jessica Chen, Sierra
597 Conway, Floreana Cordova, Xiuru Dai, Semra Palali Delen, Yavuz Delen, Tessa Durham-
598 Brooks, Samuel Eastman, Alex Enerson, Ashley Foltz, Nick Friedman, Cierra Goerish, Wihib
599 Hankore, Davron Hanley, Aris Hino, Chun Yin Ho, J. Preston Hurst, Kylie Irene, Panya Kim,
600 Nataniel Korth, Courtney Krsnak, Enzo Lamontia, Zhikai Liang, Xiangdong Liu, Angelique
601 Malcolm, Rajan Mediratta, Chenyong Miao, Xiaoxi Meng, Levi Nigro, Alejandro Pages, Connor
602 Pedersen, Nathaniel Pester, Sam Polk, Raghuprakash Kastoori Ramamurthy, Eric Rodene,
603 Daniel Santano de Carvalho, Emma Sheridan, Aris Shino, Isabel Sigmon, Taylor Stratman,
604 Guangchao Sun, Michael Tross, Misty Wehling, Florian Wurtele and Zhikai Yang.

605 Competing interests

606 The authors declare that they have no competing interests.

607 References

608

609 Bakker, P.A.H.M., Berendsen, R.L., Doornbos, R.F., Wintermans, P.C.A., and Pieterse, C.M.J. (2013).
610 The rhizosphere revisited: root microbiomics. Frontiers in Plant Science *4*.
611 Bates, D., Mächler, M., Bolker, B., and Walker, S. (2015). Fitting Linear Mixed-Effects Models Using lme4.
612 Journal of Statistical Software *67*, 1–48.

Baudoin, E., Benizri, E., and Guckert, A. (2003). Impact of artificial root exudates on the bacterial community structure in bulk soil and maize rhizosphere. Soil Biology and Biochemistry *35*, 1183–1192.

Beilsmith, K., Thoen, M.P.M., Brachi, B., Gloss, A.D., Khan, M.H., and Bergelson, J. (2019). Genome-wide association studies on the phyllosphere microbiome: Embracing complexity in host-microbe interactions. Plant J *97*, 164–181.

Bergelson, J., Mittelstrass, J., and Horton, M.W. (2019). Characterizing both bacteria and fungi improves understanding of the Arabidopsis root microbiome. Sci Rep *9*, 24.

Bernabeu, P.R., Pistorio, M., Torres-Tejerizo, G., Estrada-De los Santos, P., Galar, M.L., Boiardi, J.L., and Luna, M.F. (2015). Colonization and plant growth-promotion of tomato by Burkholderia tropica. Scientia Horticulturae *191*, 113–120.

Bray, A.L., and Topp, C.N. (2018). The Quantitative Genetic Control of Root Architecture in Maize. Plant and Cell Physiology *59*, 1919–1930.

Brisson, V.L., Schmidt, J.E., Northen, T.R., Vogel, J.P., and Gaudin, A.C.M. (2019). Impacts of Maize Domestication and Breeding on Rhizosphere Microbial Community Recruitment from a Nutrient Depleted Agricultural Soil. Sci Rep *9*, 15611.

Bukowski, R., Guo, X., Lu, Y., Zou, C., He, B., Rong, Z., Wang, B., Xu, D., Yang, B., Xie, C., et al. (2018). Construction of the third-generation Zea mays haplotype map. GigaScience *7*.

Callahan, B.J., Sankaran, K., Fukuyama, J.A., McMurdie, P.J., and Holmes, S.P. (2016a). Bioconductor Workflow for Microbiome Data Analysis: from raw reads to community analyses. F1000Research *5*, 1492.

Callahan, B.J., McMurdie, P.J., Rosen, M.J., Han, A.W., Johnson, A.J.A., and Holmes, S.P. (2016b). DADA2: High-resolution sample inference from Illumina amplicon data. Nature Methods *13*, 581–583.

Cao, P., Lu, C., and Yu, Z. (2018). Historical nitrogen fertilizer use in agricultural ecosystems of the contiguous United States during 1850–2015: application rate, timing, and fertilizer types. Earth System Science Data *10*, 969–984.

Chang, C.C., Chow, C.C., Tellier, L.C., Vattikuti, S., Purcell, S.M., and Lee, J.J. (2015). Second-generation PLINK: rising to the challenge of larger and richer datasets. Gigascience *4*, s13742-015.

Chen, R., Tian, M., Wu, X., and Huang, Y. (2011). Differential global gene expression changes in response to low nitrogen stress in two maize inbred lines with contrasting low nitrogen tolerance. Genes

Genom *33*, 491–497.

Ciampitti, I.A., Murrell, S.T., Camberato, J.J., Tuinstra, M., Xia, Y., Friedemann, P., and Vyn, T.J. (2013). Physiological Dynamics of Maize Nitrogen Uptake and Partitioning in Response to Plant Density and Nitrogen Stress Factors: II. Reproductive Phase. Crop Sci. *53*, 2588–2602.

Covarrubias-Pazaran, G. (2016). Genome-Assisted Prediction of Quantitative Traits Using the R Package sommer. PLoS ONE *11*, e0156744.

Dardanelli, M.S., Manyani, H., González-Barroso, S., Rodríguez-Carvajal, M.A., Gil-Serrano, A.M., Espuny, M.R., López-Baena, F.J., Bellogín, R.A., Megías, M., and Ollero, F.J. (2010). Effect of the presence of the plant growth promoting rhizobacterium (PGPR) Chryseobacterium balustinum Aur9 and salt stress in the pattern of flavonoids exuded by soybean roots. Plant Soil *328*, 483–493.

Deng, S., Caddell, D.F., Xu, G., Dahlen, L., Washington, L., Yang, J., and Coleman-Derr, D. (2021). Genome wide association study reveals plant loci controlling heritability of the rhizosphere microbiome. ISME J.

Doornbos, R.F., van Loon, L.C., and Bakker, P.A.H.M. (2012). Impact of root exudates and plant defense signaling on bacterial communities in the rhizosphere. A review. Agron. Sustain. Dev. *32*, 227–243.

Eida, A.A., Hirt, H., and Saad, M.M. (2017). Challenges Faced in Field Application of Phosphate-Solubilizing Bacteria. In Rhizotrophs: Plant Growth Promotion to Bioremediation, S. Mehnaz, ed. (Singapore: Springer Singapore), pp. 125–143.

Flint-Garcia, S.A., Thuillet, A.-C., Yu, J., Pressoir, G., Romero, S.M., Mitchell, S.E., Doebley, J., Kresovich, S., Goodman, M.M., and Buckler, E.S. (2005). Maize association population: a high-resolution platform for quantitative trait locus dissection: High-resolution maize association population. The Plant Journal *44*, 1054–1064.

Garbeva, P., van Elsas, J.D., and van Veen, J.A. (2008). Rhizosphere microbial community and its s fine-scale and growth variation phenotypes in roots of adult-stage maize (Zea mays L.) in response to low nitrogen stress: Nitrogen stress on maize roots. Plant, Cell & Environment *34*, 2122–2137.

Ge, Y., Atefi, A., Zhang, H., Miao, C., Ramamurthy, R.K., Sigmon, B., Yang, J., and Schnable, J.C. (2019). High-throughput analysis of leaf physiological and chemical traits with VIS–NIR–SWIR spectroscopy: a case study with a maize diversity panel. Plant Methods *15*, 1–12.

669 Gohl, D.M., Vangay, P., Garbe, J., MacLean, A., Hauge, A., Becker, A., Gould, T.J., Clayton, J.B.,
670 Johnson, T.J., Hunter, R., et al. (2016). Systematic improvement of amplicon marker gene methods for
671 increased accuracy in microbiome studies. Nature Biotechnology *34*, 942–949.
672 Gomes, E.A., Lana, U.G.P., Quensen, J.F., de Sousa, S.M., Oliveira, C.A., Guo, J., Guimarães, L.J.M.,
673 and Tiedje, J.M. (2018). Root-Associated Microbiome of Maize Genotypes with Contrasting Phosphorus
674 Use Efficiency. Phytobiomes Journal *2*, 129–137.
675 Haase, S., Neumann, G., Kania, A., Kuzyakov, Y., Römheld, V., and Kandeler, E. (2007). Elevation of
676 atmospheric CO2 and N-nutritional status modify nodulation, nodule-carbon supply, and root exudation of
677 Phaseolus vulgaris L. Soil Biology and Biochemistry *39*, 2208–2221.
678 Haegele, J.W., Cook, K.A., Nichols, D.M., and Below, F.E. (2013). Changes in Nitrogen Use Traits
679 Associated with Genetic Improvement for Grain Yield of Maize Hybrids Released in Different Decades.
680 Crop Science *53*, 1256–1268.
681 Hussain, S.S., Mehnaz, S., and Siddique, K.H.M. (2018). Harnessing the Plant Microbiome for Improved
682 Abiotic Stress Tolerance. In Plant Microbiome: Stress Response, D. Egamberdieva, and P. Ahmad, eds.
683 (Singapore: Springer Singapore), pp. 21–43.
684 Jiao, Y., Peluso, P., Shi, J., Liang, T., Stitzer, M.C., Wang, B., Campbell, M.S., Stein, J.C., Wei, X., Chin,
685 C.-S., et al. (2017). Improved maize reference genome with single-molecule technologies. Nature *546*,
686 524–527.
687 Kaur, T., Rana, K.L., Kour, D., Sheikh, I., Yadav, N., Kumar, V., Yadav, A.N., Dhaliwal, H.S., and Saxena,
688 A.K. (2020). Microbe-mediated biofortification for micronutrients: Present status and future challenges. In
689 New and Future Developments in Microbial Biotechnology and Bioengineering, (Elsevier), pp. 1–17.
690 Kremling, K.A.G., Chen, S.-Y., Su, M.-H., Lepak, N.K., Romay, M.C., Swarts, K.L., Lu, F., Lorant, A.,
691 Bradbury, P.J., and Buckler, E.S. (2018). Dysregulation of expression correlates with rare-allele burden
692 and fitness loss in maize. Nature *555*, 520–523.
693 Kumar, P., Dubey, R.C., and Maheshwari, D.K. (2012). Bacillus strains isolated from rhizosphere showed
694 plant growth promoting and antagonistic activity against phytopathogens. Microbiological Research *167*,
695 493–499.
696 Kurepin, L.V., Park, J.M., Lazarovits, G., and Bernards, M.A. (2015). Burkholderia phytofirmans-induced

shoot and root growth promotion is associated with endogenous changes in plant growth hormone levels. Plant Growth Regul *75*, 199–207.

Liao, Y., Smyth, G.K., and Shi, W. (2019). The R package Rsubread is easier, faster, cheaper and better for alignment and quantification of RNA sequencing reads. Nucleic Acids Research *47*, e47–e47.

Limborg, M., and Heeb, P. (2018). Special Issue: Coevolution of Hosts and Their Microbiome. Genes *9*, 549.

Liu, Y.-X., Qin, Y., Chen, T., Lu, M., Qian, X., Guo, X., and Bai, Y. (2021). A practical guide to amplicon and metagenomic analysis of microbiome data. Protein Cell *12*, 315–330.

Love, M.I., Huber, W., and Anders, S. (2014). Moderated estimation of fold change and dispersion for RNA-seq data with DESeq2. Genome Biology *15*.

Madhaiyan, M., Poonguzhali, S., Lee, J.-S., Senthilkumar, M., Lee, K.C., and Sundaram, S. (2010). Mucilaginibacter gossypii sp. nov. and Mucilaginibacter gossypiicola sp. nov., plant-growth-promoting bacteria isolated from cotton rhizosphere soils. INTERNATIONAL JOURNAL OF SYSTEMATIC AND EVOLUTIONARY MICROBIOLOGY *60*, 2451–2457.

Meier, M.A., Lopez-Guerrero, M.G., Guo, M., Schmer, M.R., Herr, J.R., Schnable, J.C., Alfano, J.R., and Yang, J. (2021). Rhizosphere Microbiomes in a Historical Maize/Soybean Rotation System respond to Host Species and Nitrogen Fertilization at Genus and Sub-genus Levels. Appl Environ Microbiol AEM.03132-20, aem;AEM.03132-20v1.

Mönchgesang, S., Strehmel, N., Schmidt, S., Westphal, L., Taruttis, F., Müller, E., Herklotz, S., Neumann, S., and Scheel, D. (2016). Natural variation of root exudates in Arabidopsis thaliana-linking metabolomic and genomic data. Sci Rep *6*, 29033.

Nunes da Rocha, U., Plugge, C.M., George, I., van Elsas, J.D., and van Overbeek, L.S. (2013). The Rhizosphere Selects for Particular Groups of Acidobacteria and Verrucomicrobia. PLoS ONE *8*, e82443.

Otieno, N., Lally, R.D., Kiwanuka, S., Lloyd, A., Ryan, D., Germaine, K.J., and Dowling, D.N. (2015). Plant growth promotion induced by phosphate solubilizing endophytic Pseudomonas isolates. Frontiers in Microbiology *6*, 745.

Peiffer, J.A., Spor, A., Koren, O., Jin, Z., Tringe, S.G., Dangl, J.L., Buckler, E.S., and Ley, R.E. (2013). Diversity and heritability of the maize rhizosphere microbiome under field conditions. Proceedings of the

National Academy of Sciences *110*, 6548–6553.

Pérez-Jaramillo, J.E., Mendes, R., and Raaijmakers, J.M. (2016). Impact of plant domestication on rhizosphere microbiome assembly and functions. Plant Mol Biol *90*, 635–644.

Piromyou, P., Buranabanyat, B., Tantasawat, P., Tittabutr, P., Boonkerd, N., and Teaumroong, N. (2011). Effect of plant growth promoting rhizobacteria (PGPR) inoculation on microbial community structure in rhizosphere of forage corn cultivated in Thailand. European Journal of Soil Biology *47*, 44–54.

Preston, G.M. (2004). Plant perceptions of plant growth-promoting *Pseudomonas*. Phil. Trans. R. Soc. Lond. B *359*, 907–918.

Rice, B.R., Fernandes, S.B., and Lipka, A.E. (2020). Multi-Trait Genome-Wide Association Studies Reveal Loci Associated with Maize Inflorescence and Leaf Architecture. Plant and Cell Physiology *61*, 1427–1437.

Rodene, E., Xu, G., Delen, S.P., Smith, C., Ge, Y., Schnable, J., and Yang, J. (2021). A UAV-based high-throughput phenotyping approach to assess time-series nitrogen responses and identify traits associated genetic components in maize (Plant Biology).

Saleem, M., Hu, J., and Jousset, A. (2019). More Than the Sum of Its Parts: Microbiome Biodiversity as a Driver of Plant Growth and Soil Health. Annu. Rev. Ecol. Evol. Syst. *50*, 145–168.

Sasse, J., Martinoia, E., and Northen, T. (2018). Feed Your Friends: Do Plant Exudates Shape the Root Microbiome? Trends in Plant Science *23*, 25–41.

Schnable, P.S., Ware, D., Fulton, R.S., Stein, J.C., Wei, F., Pasternak, S., Liang, C., Zhang, J., Fulton, L., Graves, T.A., et al. (2009). The B73 Maize Genome: Complexity, Diversity, and Dynamics. Science *326*, 1112–1115.

Sessitsch, A., Pfaffenbichler, N., and Mitter, B. (2019). Microbiome Applications from Lab to Field: Facing Complexity. Trends in Plant Science *24*, 194–198.

Sharma, S., Kumar, S., Khajuria, A., Ohri, P., Kaur, R., and Kaur, R. (2020). Biocontrol potential of chitinases produced by newly isolated Chitinophaga sp. S167. World J Microbiol Biotechnol *36*, 90.

Singer, E., Vogel, J.P., Northen, T., Mungall, C.J., and Juenger, T.E. (2021). Novel and Emerging Capabilities that Can Provide a Holistic Understanding of the Plant Root Microbiome. Phytobiomes Journal *5*, 122–132.

Singh, A.V., Chandra, R., and Goel, R. (2013). Phosphate solubilization by *Chryseobacterium* sp. and their combined effect with N and P fertilizers on plant growth promotion. Archives of Agronomy and Soil Science *59*, 641–651.

Sutherland, J., Bell, T., Trexler, R.V., Carlson, J.E., and Lasky, J.R. (2021). Host genomic influence on bacterial composition in the switchgrass rhizosphere (Plant Biology).

Van Deynze, A., Zamora, P., Delaux, P.-M., Heitmann, C., Jayaraman, D., Rajasekar, S., Graham, D., Maeda, J., Gibson, D., Schwartz, K.D., et al. (2018). Nitrogen fixation in a landrace of maize is supported by a mucilage-associated diazotrophic microbiota. PLoS Biol *16*, e2006352.

Van Gerrewey, T., Vandecruys, M., Ameloot, N., Perneel, M., Van Labeke, M.-C., Boon, N., and Geelen, D. (2020). Microbe-Plant Growing Media Interactions Modulate the Effectiveness of Bacterial Amendments on Lettuce Performance Inside a Plant Factory with Artificial Lighting. Agronomy *10*, 1456.

Vandenkoornhuyse, P., Quaiser, A., Duhamel, M., Le Van, A., and Dufresne, A. (2015). The importance of the microbiome of the plant holobiont. New Phytol *206*, 1196–1206.

Wallace, J.G., Kremling, K.A., Kovar, L.L., and Buckler, E.S. (2018). Quantitative Genetics of the Maize Leaf Microbiome. Phytobiomes Journal *2*, 208–224.

Walters, W.A., Jin, Z., Youngblut, N., Wallace, J.G., Sutter, J., Zhang, W., González-Peña, A., Peiffer, J., Koren, O., Shi, Q., et al. (2018). Large-scale replicated field study of maize rhizosphere identifies heritable microbes. Proceedings of the National Academy of Sciences 201800918.

Woodhouse, M.R., Cannon, E.K., Portwood, J.L., Harper, L.C., Gardiner, J.M., Schaeffer, M.L., and Andorf, C.M. (2021). A pan-genomic approach to genome databases using maize as a model system. BMC Plant Biol *21*, 385.

Xi, N., Bloor, J.M.G., and Chu, C. (2020). Soil microbes alter seedling performance and biotic interactions under plant competition and contrasting light conditions. Annals of Botany *126*, 1089–1098.

Yadav, A.N., Kumar, V., Dhaliwal, H.S., Prasad, R., and Saxena, A.K. (2018). Microbiome in Crops: Diversity, Distribution, and Potential Role in Crop Improvement. In Crop Improvement Through Microbial Biotechnology, (Elsevier), pp. 305–332.

Yee, M.O., Kim, P., Li, Y., Singh, A.K., Northen, T.R., and Chakraborty, R. (2021). Specialized Plant Growth Chamber Designs to Study Complex Rhizosphere Interactions. Front. Microbiol. *12*, 625752.

Yilmaz, P., Parfrey, L.W., Yarza, P., Gerken, J., Pruesse, E., Quast, C., Schweer, T., Peplies, J., Ludwig, W., and Glöckner, F.O. (2014). The SILVA and “All-species Living Tree Project (LTP)” taxonomic frameworks. Nucl. Acids Res. *42*, D643–D648.

Yu, P., He, X., Baer, M., Beirinckx, S., Tian, T., Moya, Y.A.T., Zhang, X., Deichmann, M., Frey, F.P., Bresgen, V., et al. (2021). Plant flavones enrich rhizosphere Oxalobacteraceae to improve maize performance under nitrogen deprivation. Nat. Plants *7*, 481–499.

Zeng, J., de Vlaming, R., Wu, Y., Robinson, M.R., Lloyd-Jones, L.R., Yengo, L., Yap, C.X., Xue, A., Sidorenko, J., McRae, A.F., et al. (2018). Signatures of negative selection in the genetic architecture of human complex traits. Nat Genet *50*, 746–753.

Zhou, X., and Stephens, M. (2012). Genome-wide efficient mixed-model analysis for association studies. Nat Genet *44*, 821–824.

Zhu, S., Vivanco, J.M., and Manter, D.K. (2016). Nitrogen fertilizer rate affects root exudation, the rhizosphere microbiome and nitrogen-use-efficiency of maize. Applied Soil Ecology *107*, 324–333.

Appendix

Supplementary Methods

Field and experimental Design

The experimental field was divided into 4 quadrants, which were separated and surrounded by a buffer of an industrial hybrid genotype (B73xMo17) (**Figure 6**). The complete set of genotypes was planted in each quadrant where possible. Each quadrant was in turn divided into 4 split plots and a subset of the maize association panel was randomly assigned to each split plot based on the distributions of flowering time and plant height. Phenotypes were divided at the median value to create 4 flowering time / height categories: early/tall, late/tall, early/short, and late/short. Each split plot was further divided into 3 split plot blocks, and each split plot block was divided into 21 subplots in 3 ranges and 7 columns. Thus 252 subplots were available in each quadrant of the field. In each of 12 split plot blocks per quadrant, a t least one subplot was

randomly selected and assigned the hybrid genotype (B73xMo17) to be used as a check to test for differences between geographical field locations. two check genotypes (B73xMo17 and B37xMo17) were used in 2018, and a single check genotype (B73xMo17) was used in 2019. Plant growth across the field was determined uniform within quadrants using the checks as reported in a sister study on the same experimental field (Rodene et al., 2022). Any subplots across the field that remained empty due to seed unavailability were filled with the check genotype as well.

In 2018, dry N fertilizer (urea) was applied to two diagonally opposed quadrants before planting at the rate of 140 kg/ha (+N treatment) while two quadrants were left unfertilized (-N treatment). In 2019, liquid N fertilizer (urea) was applied at the rate of 168 kg/ha. Both N treatments were thus represented in a northern block (NW and NE quadrants) and in a southern block (SW and SE quadrant). We assigned the blocks this way because of a 3 m increase in elevation from the north end of the field to the south end.

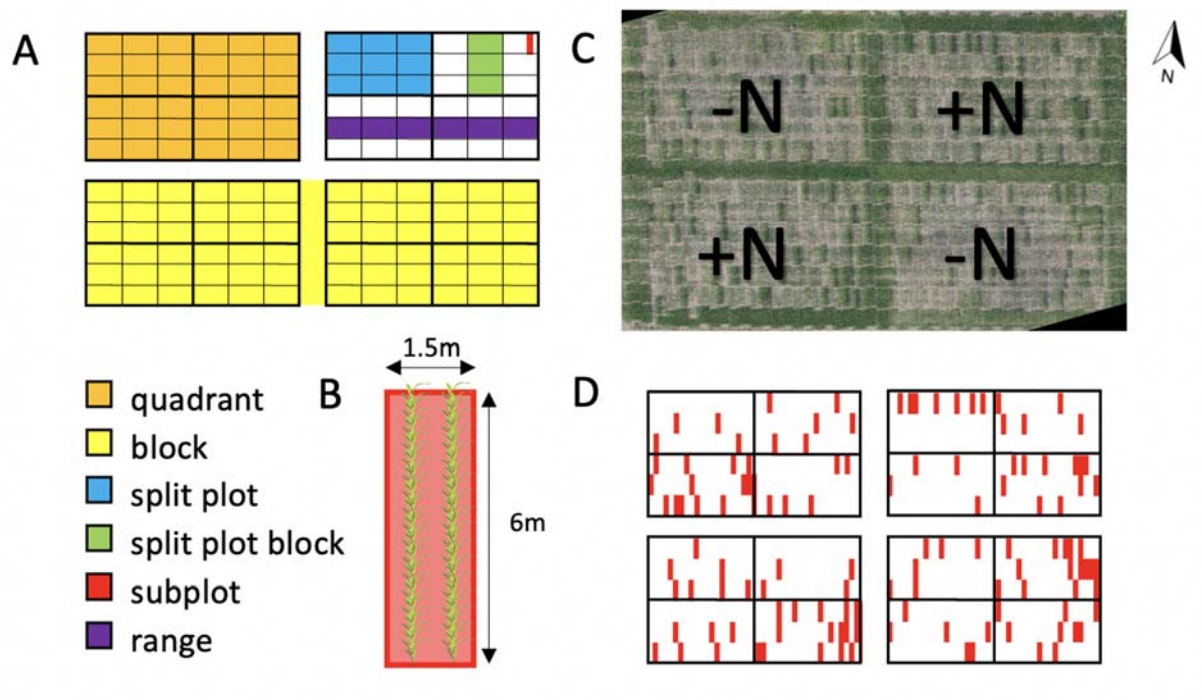

Figure 6: Field experimental design. (A) Up to 230 maize genotypes were represented in each of 4 quadrants in 2 replicate blocks. Quadrants were planted in 6 ranges and divided into 4 split plots. Each split plot was divided into 3 split plot blocks, and each split plot block was divided into 21 subplots for a total of 252 subplots per quadrant. (B) Each 1.5m (5 ft) x 6m (20 ft) subplot (experimental unit) consisted of two rows of 36 maize plants of the same genotype, with a spacing of 75 cm (30 in) between rows and 15 cm (6 in) between plants. (C) Photomosaic of the 2019 field at flowering time. N fertilizer was applied to the NE and SW quadrants before planting. (D) 128 subplots across the field (marked in red) were planted with a check genotype (B73xMo17) in order to be able to quantify and control for spatial variation.

824

825 **Rhizobiome sample preparation and sequencing**

826 In 2018, rhizosphere samples were collected from 28 genotypes. These include, B73, the
827 roothairless3 mutant of B73 (Hochholdinger et al., 2008), two check hybrids (B73xMo17 and
828 B37xMo17) and a subset of the Buckler-Goodman panel including 16 parent lines of the nested

association mapping population (NAM) described by (McMullen et al., 2009). 8 weeks after planting, 2 subsamples per genotype were collected per quadrant and 12 subsamples for checks, where each subsample was taken from the combined root material of two adjacent plants. This resulted in a total of 26*4*2 +2*4*12 = 304 samples. In 2019, rhizosphere samples were collected in triplicates from all 1008 subplots within 3 days, 8 weeks after planting, when the majority of plants had reached the tasseling stage. One of the two rows in each subplot was randomly selected, and 3 individual randomly selected plants within the row (subsamples) were sacrificed for rhizosphere collection. As a small fraction of subplots had poor germination and/or no surviving plants on the day of sampling, the final number of rhizosphere samples collected was 3009. Rhizosphere samples were placed on ice immediately after collection and shipped to the lab to be processed on the same day.

To wash the tightly adherent rhizosphere soil layer off the roots, tubes were filled up to the 40 ml mark with autoclaved PBS buffer (46 mM NaH2PO4, 60 mM Na2HPO4, 0.02% Silwet-77), and shaken horizontally at 8000 rpm for 30s. Rhizosphere suspension was filtered through a 100 µm nylon cell strainer (Celltreat Scientific Products, Pepperell, MA, USA) into a fresh 50 ml tube to capture root debris and large soil particles. Rhizosphere samples were frozen in suspension at -20°C until further processing. DNA was isolated from rhizosphere soil using the MagAttract PowerSoil DNA KF Kit (Qiagen, Hilden, Germany) and purified using the KingFisher Flex Purification System (Thermo Fisher, Waltham, MA, USA) with minor modifications to the protocol: Rhizosphere samples that were kept in suspension were thawed on ice, pelleted soil was resuspended by inverting tubes, and 500 µl soil suspension was added to the 96-well sample plates. To avoid cross contamination of wells during pipetting, plates were sealed beforehand with parafilm and the cover was pierced with the pipette tip to transfer the rhizosphere suspension into the intended well. Two plates were prepared at a time and centrifuged for 10 min at 4000 x g to pellet soil. Supernatant was carefully removed with a

multichannel pipette and 96-well plates with approximately 100-250 mg rhizosphere soil per well were frozen at -20°C until further processing. On the day of DNA isolation, the bead mill substrate was added to the frozen soil pellets, soil was thawed on ice and the remainder of the protocol was followed as per the manufacturer's instructions. We recommend this modified procedure for large numbers of samples as it is cleaner, faster, and better reproducible than scooping soil from pellets in sample tubes. Concentration of isolated DNA was measured fluorometrically with the QuantiFluor dsDNA System (Promega, Madison, WI, USA) as per the manufacturer's instructions. DNA isolation was repeated for any samples that failed to reach a concentration of at least 1 ng/µl.

A 350 bp stretch of 16S rDNA spanning the V4 region was amplified using V4_515F_Nextera (TCGTCGGCAGCGTCAGATGTGTATAAGAGACAGGTGCCAGCMGCCGCGGTAA) and V4_806R_Nextera (GTCTCGTGGGCTCGGAGATGTGTATAAGAGACAGGGACTACHVGGGTWTCTAAT) primers on several Illumina MiSeq runs. Oligonucleotide PCR blockers (PNA Bio INC, Thousand Oaks, CA, USA) targeting mitochondrial and chloroplast sequences were applied in the primary V4 amplification to reduce amplification of templates derived from the plant host. Up to 128 barcoded samples were pooled per sequencing run. In total, 304 samples in 2018 and 3009 samples in 2019 were sequenced on the same Illumina MiSeq machine.

Raw read processing and construction of microbiome dataset

Cluster computing resources at the UNL Holland Computing Center were used for computationally demanding steps. To construct the microbiome dataset, 350 bp raw sequencing reads were trimmed using filterAndTrim() at 240 bp (forward reads) and 200 bp (reverse reads), respectively. Amplicon sequence variants (ASVs) were inferred using dada() and forward and reverse reads were merged with mergePairs(). A sequence table was generated using

makeSequenceTable() and chimaeras were removed using removeBimeraDenovo(). Taxonomy was assigned to ASVs with assignTaxonomy() using the SILVA database version 138 (Yilmaz et al., 2014) as a reference. SILVA was our taxonomy of choice because it is a relatively large 16S sequence database compared to alternative databases, it is regularly maintained and updated and it is widely used in ecological research, making our results comparable to other 16S studies. (Balvočiūtė and Huson, 2017). Taxonomic training data formatted for DADA2 (silva_nr99_v138_wSpecies_train_set.fa.gz) was obtained from https://zenodo.org/record/3986799#.X3zmypNKh24, as referenced by https://benjjneb.github.io/dada2/training.html on GitHub. 16S reads and sample data were prepared in an R Phyloseq object for further processing.

Raw ASV reads were subjected to a series of filters to produce a final ASV table with biologically relevant 16S sequences:

1) Removed chimaeric 16S reads using removeBimeraDenovo()
2) Removed sequences with <20 total observations
3) Removed sequences that did not map to either Bacteria or Archaea
4) Removed chloroplast sequences
5) Removed mitochondrial sequences
6) Removed ASVs that were not observed in at least 5% (166) of all samples
7) Removed ASVs that were not observed in both years 2018 and 2019
8) Removed 53 out of 160 genera and families that had fewer than 5 unique ASVs and 7 samples with < 100 ASV counts

Step 6 resulted in 4,632 common ASVs that were detected in at least 5% of the samples, representing 120,004,239 of the raw reads. Constrained ordination and PERMANOVA analyses of the 4,632 ASVs identified a strong effect of N treatment as well as other experimental factors

907 on ASV abundance (**Figure 7**). This observation is consistent with previous observations that
908 environmental factors play an important role in determining the composition of the root
909 associated microbiome diversity (Floc'h et al., 2020; Meier et al., 2021; Schlatter et al., 2020).
910 Of the 4,632 common ASVs, 3,728 (or 80.5%) were highly abundant and observed in samples
911 collected from both the 2018 and 2019 growing seasons (step 7). Removing ASVs that could
912 not be repeatedly observed in multiple years reduced the complexity of the data set by 19.5% at
913 the cost of a 2.3% loss in diversity (Shannon diversity reduced from 6.4 to 6.3**, Figure 7 –**
914 **figure supplement 1**). Finally, removing taxa (genus or family) with less than 5 observed ASVs
915 yielded a dataset of 3,626 ASVs, 3,306 samples, and 105,745,986 total ASV counts. This final
916 core microbiome encompasses <1% of initial ASVs and ~50% of initial observations. The ASV
917 table from step 8 was converted to relative abundances and values were transformed with the
918 natural logarithm. A phylogenetic tree was constructed from the final set of 3626 ASVs using
919 mafft v. 7.404 (Katoh and Standley, 2013) for multiple alignment and fasttree v. 2.1 (Price et al.,
920 2010) and the phylogenetic tree was attached to the phyloseq object and plotted using the
921 ggtree R package (Yu, 2020).
922

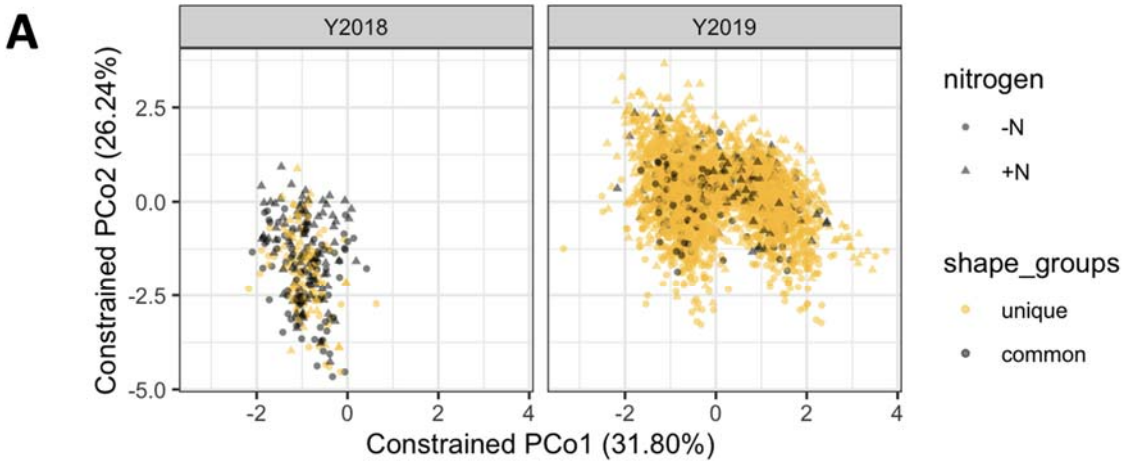

B

```
formula = dm ~ year + genotype + nitrogen + block + sp
```

	Df	SumsOfSqs	MeanSqs	F.Model	R2	Pr(>F)	
year	1	3.354	3.3540	301.32	0.06311	0.001	***
genotype	234	7.239	0.0309	2.78	0.13620	0.001	***
nitrogen	1	1.783	1.7826	160.15	0.03354	0.001	***
block	1	5.911	5.9105	531.01	0.11121	0.001	***
sp	3	0.695	0.2317	20.81	0.01308	0.001	***
spb	2	0.063	0.0314	2.82	0.00118	0.002	**
Residuals	3064	34.105	0.0111		0.64169		
Total	3306	53.148			1.00000		

Figure 7: PERMANOVA results. It was calculated from the log(relative abundance) of 4,632 ASVs. Each dot represents a sample. Genotypes common to 2018 and 2019 panel are marked in grey.

Figure 7 - figure supplement 1: **Retaining ASVs observed in both years reduces dataset complexity with minimal loss of diversity.** (A) Intermediate set of ASVs after prevalence filtering contains 4,632 ASVs, of which 904 were exclusively found in 2019. (B) Comparison of the Shannon diversity between the total set (4632 ASVs, purple) and the shared set (3728 ASVs, gold) reveals a 2.29% loss in diversity: Median(Shannon3728)/Median(Shannon4632) = 0.9771.

923

Clustering of ASVs into microbial groups

ASVs were clustered into groups of rhizosphere microbes at the family, genus, and species level using a procedure described previously (Meier et al., 2021). First, the 3,626 ASVs in the present study were grouped at the family level (the lowest taxonomic rank for which all ASVs were successfully annotated) and the phylogenetic tree derived from 16S V4 alignment was plotted alongside taxonomic annotation at the genus and species level. Because the ASVs are derived from short reads and may constitute variations not covered in the SILVA database, annotation at the genus and species level was often not possible. To close these gaps and form biologically meaningful groups of ASVs at low taxonomic ranks with better confidence, we examined the overall abundance of each ASV as well as the differential abundance in response to the N treatment alongside the sequence-based clustering. The premise here is that ASVs derived from biologically closely related individual microbes are similarly abundant in our dataset and respond similarly to the N treatment imposed on the field, in addition to similar 16S sequences due to common ancestry. An example is given in **Figure 8** with a subset of ASVs assigned to the *Burkholderiaceae* family. The plots used to determine all 150 microbial groups in this study are available in **Supplementary File 6**.

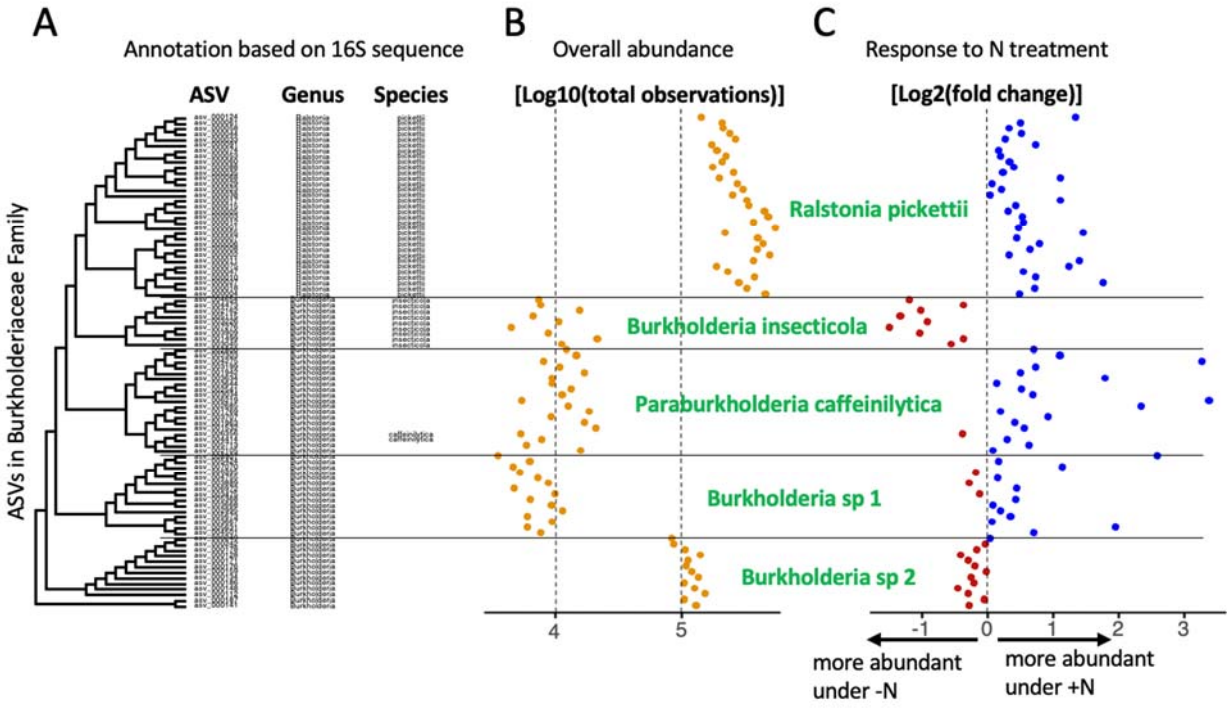

Figure 8: **Microbial groups are derived from taxonomic data and experimental data.** An example is given using a subset of the ASVs in the *Burkholderiaceae* family. (A) Phylogenetic clustering of ASVs based on 16S V4 alignment. ASVs are annotated at the genus and species level using the SILVA database. Note that for some ASVs, annotation at the species level is missing, although the phylogenetic tree suggests divergent groups at the species level. Overall abundance in the dataset (B) of each ASV and differential abundance in response to the N treatment (C) were used in tandem with sequence-based clustering to group ASVs with similar features into microbial groups at sub-genus resolution (labeled in green).

In this example, the genus *Ralstonia* constitutes a monophyletic cluster of ASVs which were all successfully assigned to the species *R. pickettii* (A). This uniform group is also reflected in relatively uniform abundance (B) and positive response to N treatment (C). On the other hand, most ASVs in the *Burkholderia* genus could not be annotated at the species level, even though the phylogeny suggests at least 4 distinct groups below the genus level. The first group, *Burkholderia insecticola* was identified at the species level without fail and once again, this is reflected in uniform abundances as well as a

consistently negative response to N treatment. Within the next cluster two ASVs are assigned to *Paraburkholderia caffeinilytica*, and we assigned all other ASVs in the same cluster to the same species because they showed consistent abundance and response to treatment. In the remaining two clusters, no ASVs could be annotated at the species level, hence we assigned a number to the unassigned species (*Burkholderia sp 1* and *sp 2*). Experimental data confirms that the two clusters should be treated as separate microbial groups because *Burkholderia sp 2* is roughly 10 times as abundant as *Burkholderia sp 1* and we observe opposite responses to N treatment.

941

942 **Heritability estimation**

943 To calculate heritability (h2), read counts from 3 subsamples were pooled for each subplot.
944 Combined counts were then normalized by converting to relative abundance and subsequent
945 natural log transformation, which yielded a subplot-level measure of microbial abundance,
946 replicated in 2 blocks. The following linear mixed model was used with all random effects: Y =
947 genotype + block + error. Y is the log-transformed relative abundance of each microbial group in
948 each subplot-level sample, the blocks and subplots are as outlined in (**Figure 6**). Heritability
949 was tested for significance using a permutation test in which microbial abundance data for each
950 trait was shuffled and heritability calculated anew 1000 times. p-values indicating heritability
951 were calculated by tallying the number of permutation h2 scores exceeding the observed h2 and
952 dividing by the number of permutations. Traits with a p-value < 0.05 were deemed “heritable”
953 under either or both N treatments.

954

955 **Estimation of genetic architecture parameters**

956 SNPs in high linkage disequilibrium (LD) were pruned using the “indep-pairwise” command of
957 with a LD threshold of r2 = 0.1. In the GCTB analysis, the BayesS model was used with the
958 chain length of 410,000 and burnin 10,000. One example command used for the GCTB analysis

is “gctb –bfile 282_GCTB_G --pheno gctb_blup_stdN_150_tax_groups.txt --mpheno 28 --out Results_HN/asv_000013 --bayes S --pi 0.05 --hsq 0.5 --S 0 --wind 0.1 --chain-length 410000 --burn-in 10000”.

Genome-wide association study

GWAS was performed using GEMMA 0.98 (Zhou and Stephens, 2012) with the following parameters: gemma-0.98 -bfile {snp_file} -k {kinship_matrix} -c {pca_file} -p {traits_file} -lmm 1 -n {trait_num} -outdir {outdir_path} -o T{trait_num} -miss 0.9 -r2 1 -hwe 0 -maf 0.01'). Blup values were summarized in a trait matrix (214 genotypes x 150 traits) for all 150 rhizobiome traits and for all 214 maize genotypes for which high quality SNP data was available. To conserve disk space, SNP information was only retained in each ASV if a response at p_wald < 10–2 was observed. To identify genomic loci with high counts of significant SNPs, the genome was split into bins of 10 kbp, and the number of significant SNP signals at a threshold of p_wald < 10–5 was counted for each bin.

Datasets

The datasets generated in this study are available as supplementary datasets:

Supplementary File 1: Feature table (3,306 samples by 3,626 ASVs) from which our results were generated, alongside the sample metadata collected in this study.

Supplementary File 2: Taxonomically annotated list of 3,626 16S sequences that comprise the core maize microbiome used for this analysis and may serve as a reference to identify the same maize-associated ASVs in future experiments.

Supplementary File 3: List of the 150 microbial groups defined in this study alongside relevant summary statistics, such as abundance, heritability, selection coefficients, and correlations with plant traits under both N treatments.

Supplementary File 4: List of 229 Buckler-Goodman maize genotypes with the corresponding measurements of all 17 plant and 150 rhizobiome traits analyzed here under both N treatments. Sample-level data is published for aerial imaging (Rodene et al., 2022).

Supplementary File 5: List of 622 plant loci (10 kb genomic regions) that exhibit significant association with one or more microbial groups, including the IDs of nearby (+/- 10 kb) genes.

Supplementary File 6: Plots of phylogeny, abundance and response to N treatment for all microbial families present in this dataset, with clustering of ASVs into the microbial groups used here.

Figure Supplements

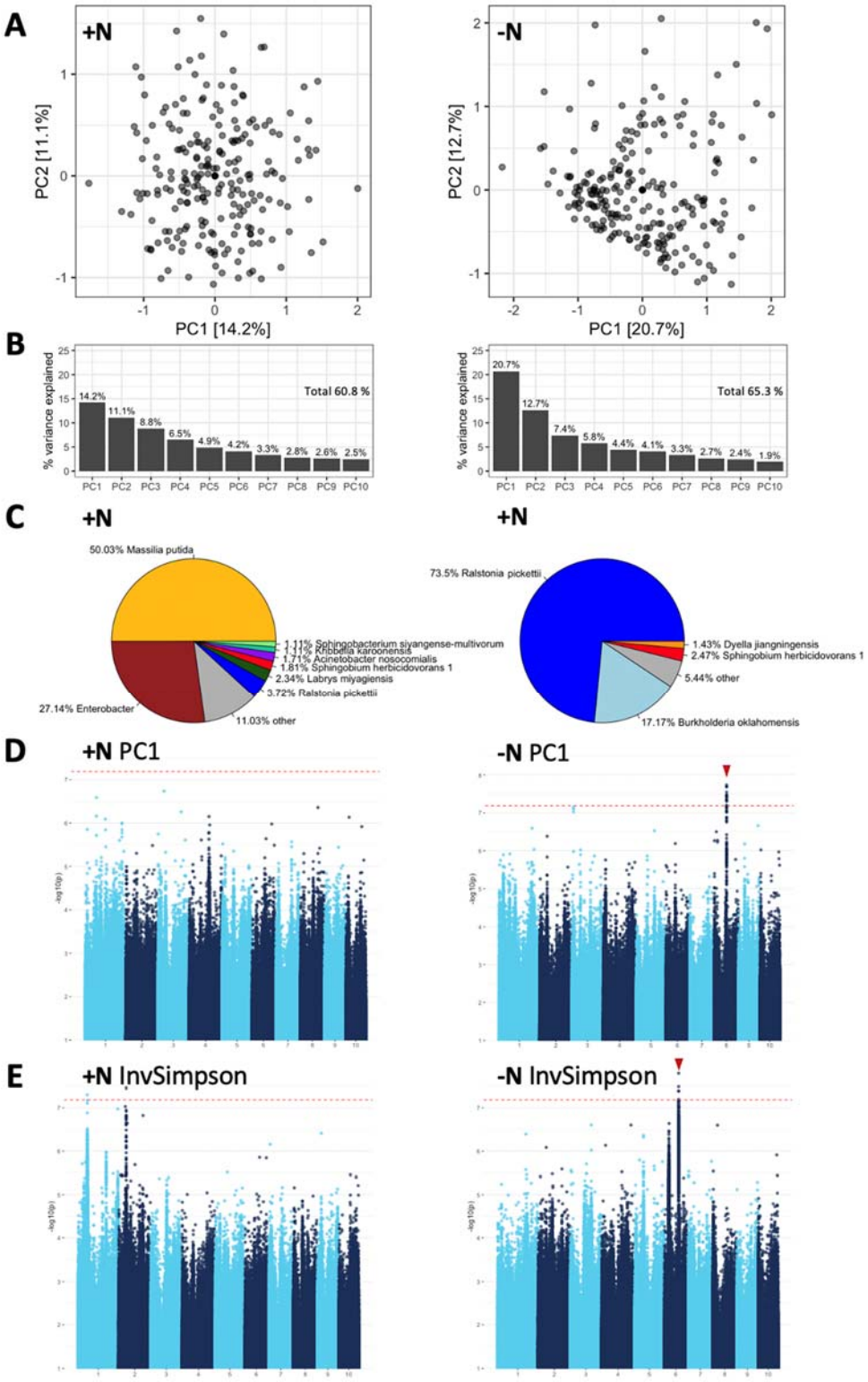

Figure 1 – figure supplement 1: GWAS of high-level rhizobiome traits:

(A, B) The first 10 principal components were calculated for both the high N (left) and low N (right) treatment using the best linear unbiased prediction (BLUPs) of the log(relative abundance) of 3618 ASVs in 230 maize genotypes. Total variance explained was 60.8% for +N and 65.3% for -N.

(C) The largest contributors to PC1 differed between the two experimental conditions. Microbial groups that account for at least 1% of total variance are annotated in the pie charts.

(D, E). Notable GWAS signals above the significance threshold (dashed red line) were observed in the -N treatment for PC1 and the InvSimpson diversity metric (red arrows), indicating genomic loci that affect high-level metrics of the rhizobiome. The other PCs and diversity metrics had no strong GWAS signals and were not shown.

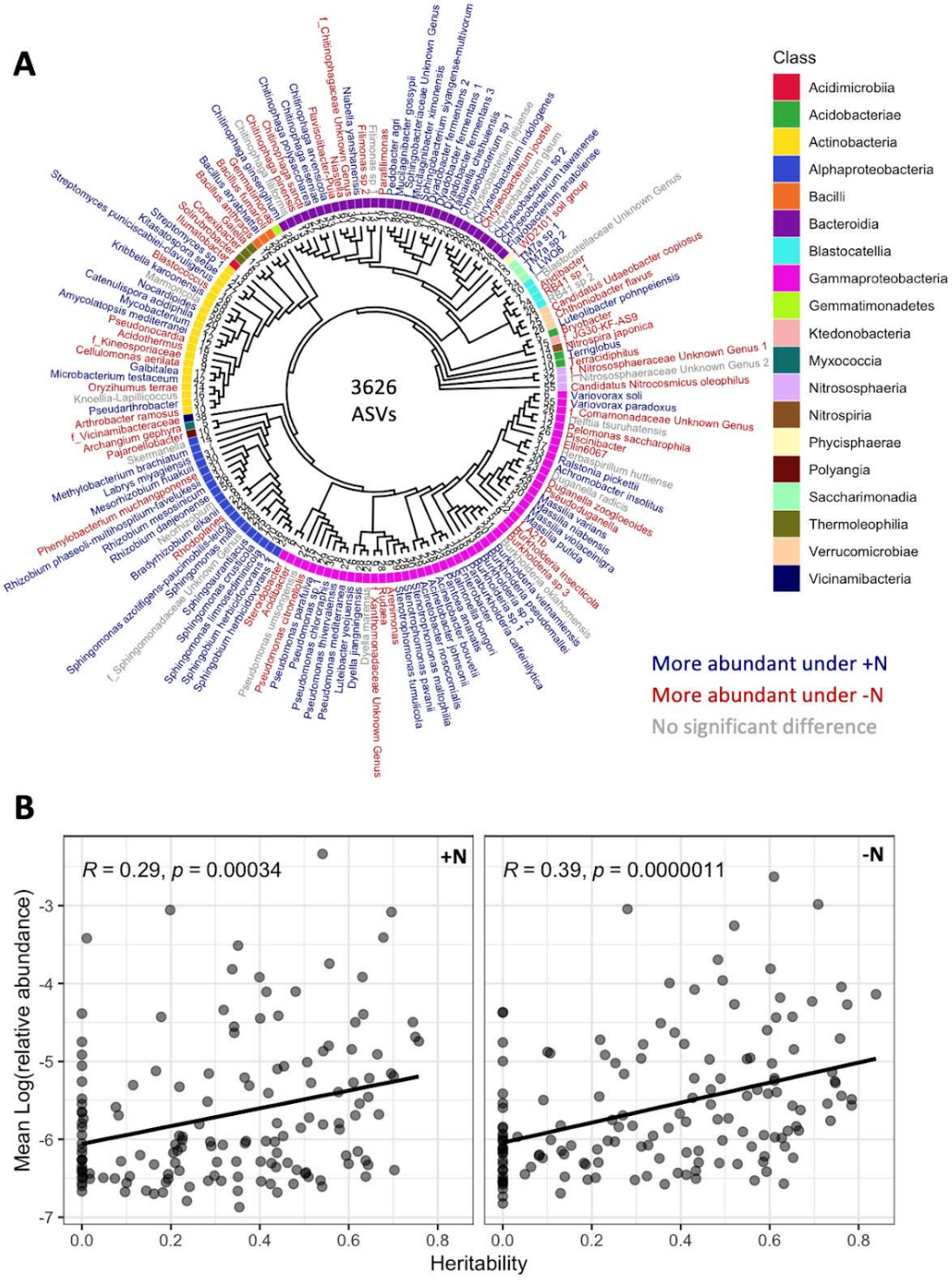

Figure 1 – figure supplement 2: Abundance and heritability of 150 microbial groups.

(A) Phylogenetic tree of 150 microbial groups. Colors indicate differential abundance between the +N and -N treatment.

(B) The mean abundance (mean BLUP of log(relative abundance) across 230 maize genotypes) of each microbial group was plotted against the heritability score in the +N and -N treatment. A positive correlation is observed in both environments, indicating that more abundant microbes in the rhizosphere also tend to be more heritable.

A

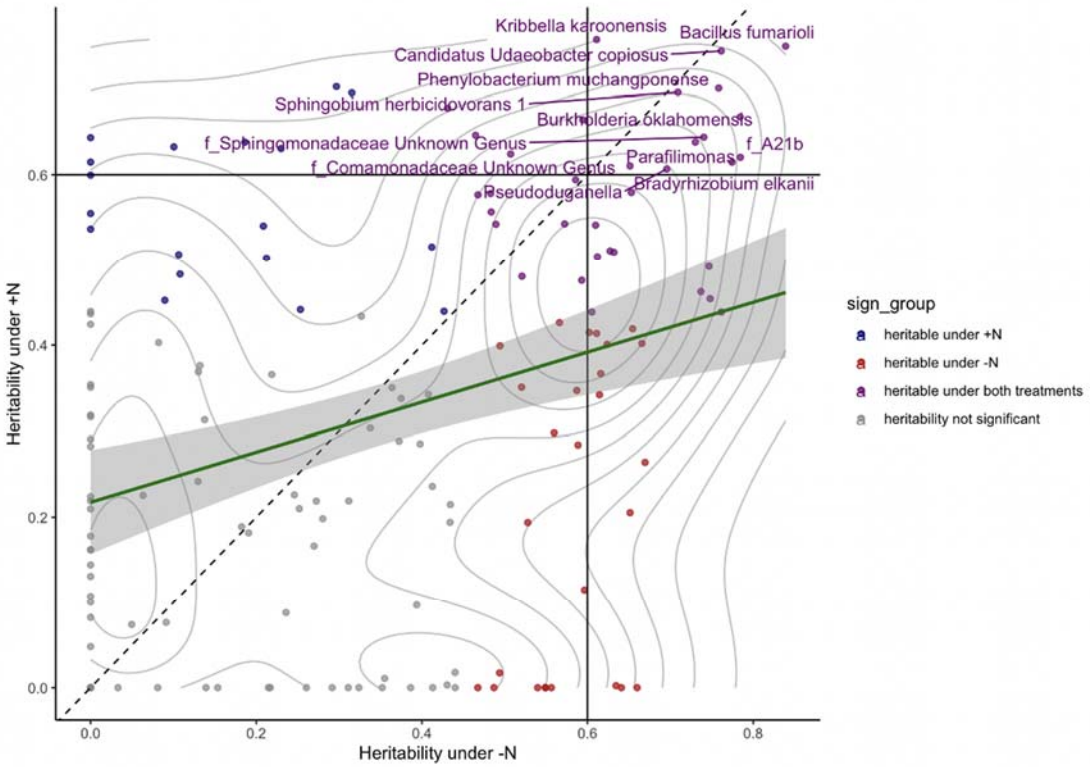

B

Phylum	Class	Order	Family	tax_group
Verrucomicrobiota	Verrucomicrobiae	Chthoniobacterales	Chthoniobacteraceae	Candidatus Udaeobacter copiosus
Proteobacteria	Alphaproteobacteria	Sphingomonadales	Sphingomonadaceae	Sphingobium herbicidovorans 1
Proteobacteria	Alphaproteobacteria	Sphingomonadales	Sphingomonadaceae	f_Sphingomonadaceae Unknown Genus
Proteobacteria	Alphaproteobacteria	Rhizobiales	Xanthobacteraceae	Bradyrhizobium elkanii
Proteobacteria	Alphaproteobacteria	Caulobacterales	Caulobacteraceae	Phenylobacterium muchangponense
Proteobacteria	Gammaproteobacteria	Burkholderiales	Oxalobacteraceae	Pseudoduganella
Proteobacteria	Gammaproteobacteria	Burkholderiales	Comamonadaceae	f_Comamonadaceae Unknown Genus
Proteobacteria	Gammaproteobacteria	Burkholderiales	A21b	f_A21b
Proteobacteria	Gammaproteobacteria	Burkholderiales	Burkholderiaceae	Burkholderia oklahomensis
Firmicutes	Bacilli	Bacillales	Bacillaceae	Bacillus fumarioli
Bacteroidota	Bacteroidia	Chitinophagales	Chitinophagaceae	Parafilimonas
Actinobacteriota	Actinobacteria	Propionibacteriales	Nocardioidaceae	Kribbella karoonensis

Figure 1 – figure supplement 3: Annotations of heritable microbial groups. (A) The 12 most heritable microbial groups with heritability > 0.6 (drawn lines) under both N conditions were annotated by name. (B) Taxonomy of the 12 most heritable groups.

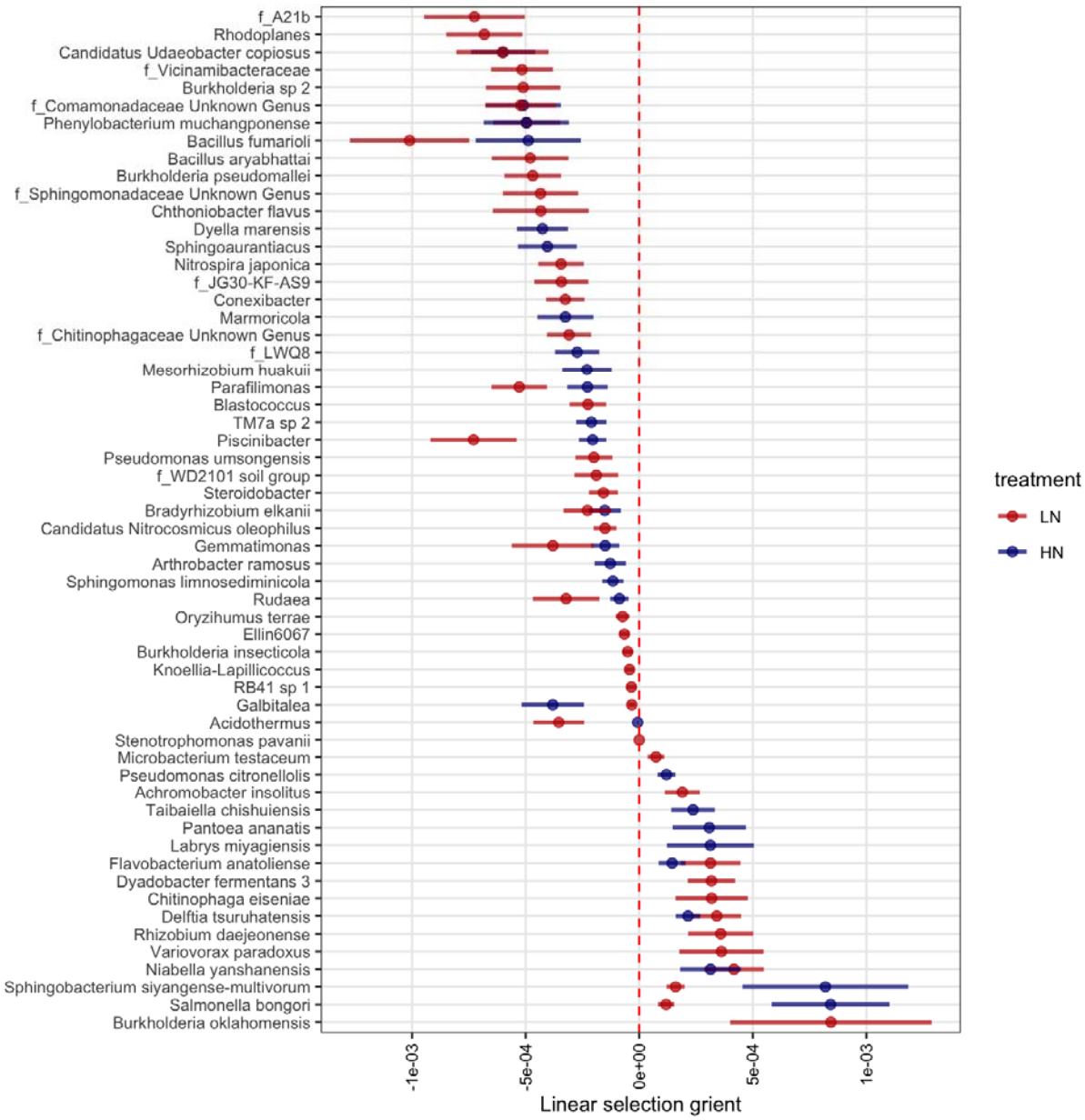

Figure 2 – figure supplement 1: Rhizobiome traits exhibit significant linear selection gradients (bootstrapping p-value < 0.05) under +N and -N treatments

1002

1003

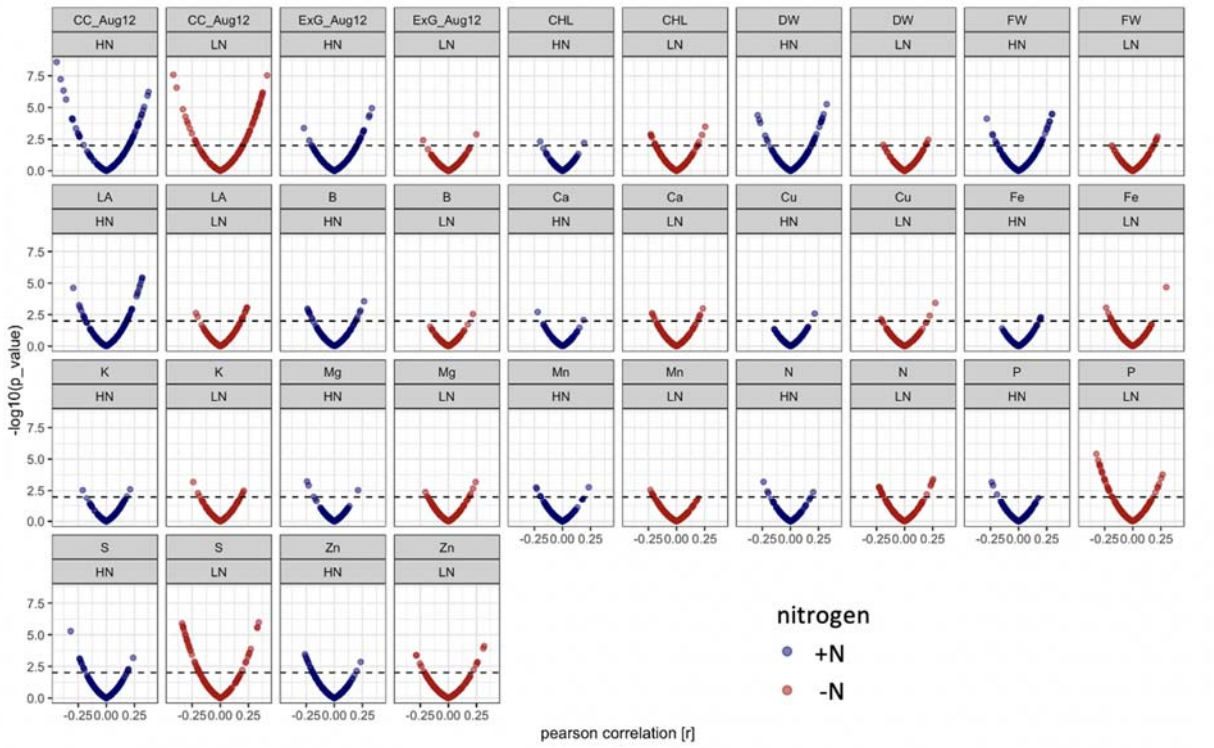

Figure 4 - figure supplement 1: Correlation of microbe abundance with 17 agronomic and micronutrient traits under +N (blue) and -N (red) conditions. Each dot represents one of 150 rhizobiome traits. X axis shows correlation with agronomic trait (r value), y axis shows significance, dashed line shows p=0.01 level of significance. CC_Aug12, EXG_Aug12: canopy coverage and excess green index measured on Aug. 12, 2019; CHL: chlorophyll content, DW: dry weight, FW: fresh weight, LA: leaf area.

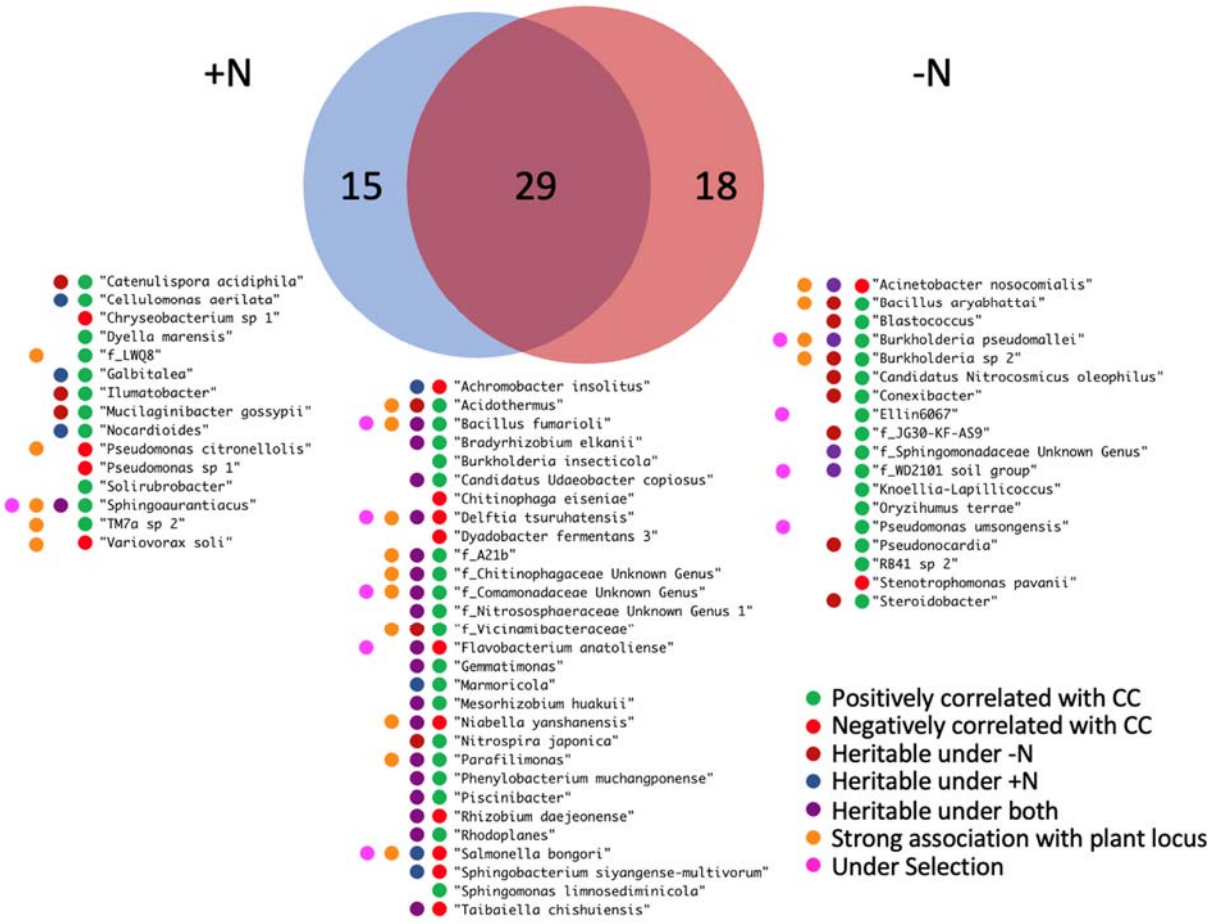

Figure 4 - figure supplement 2: Microbial traits that correlate with canopy coverage.

Venn diagram shows a total 62 microbial traits that correlate with canopy coverage either under +N, -N or both treatments. For the 62 listed rhizobiome traits, colored dots summarize various statistics that indicate association with the host plant genetics and performance.

1004

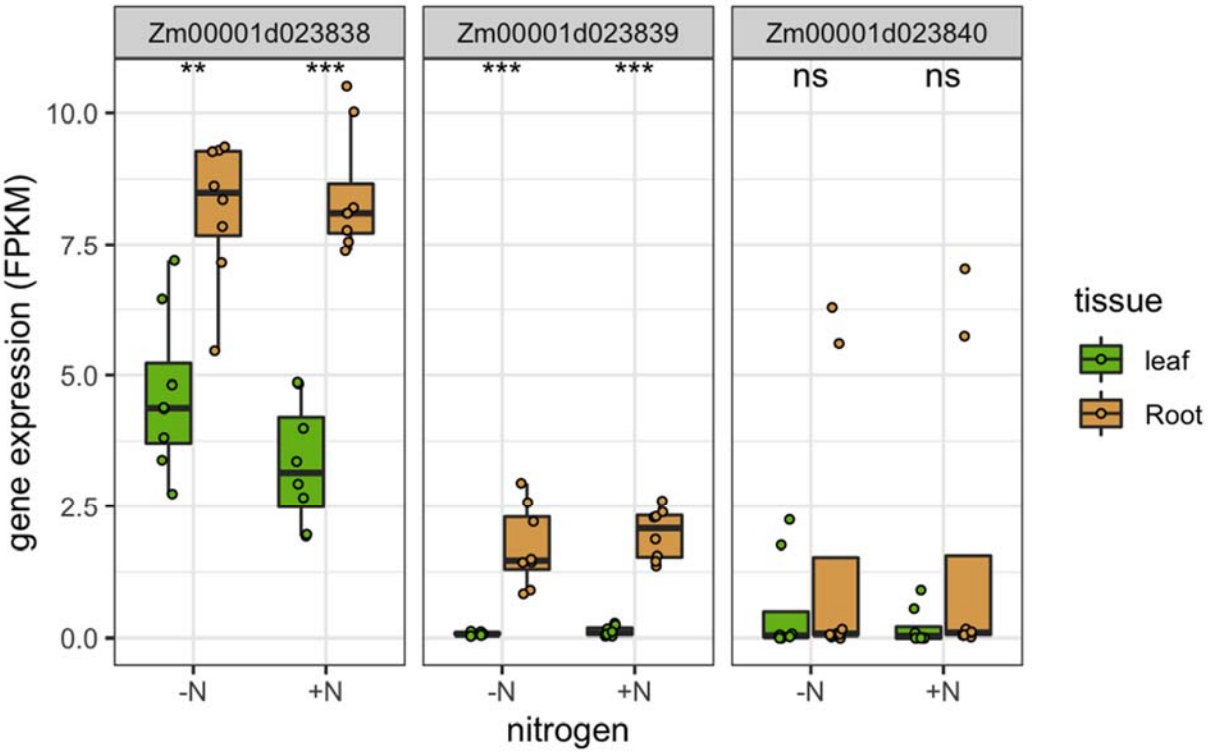

Figure 5 – figure supplement 1: Genes at MAPL are preferentially expressed in roots.

Gene expression in leaf tissue vs roots of three genes at chr 10 locus in main text **Figure 5**. Maize genotypes are the same as in main text **Figure 3C**. Genes Zm00001d023838 and Zm00001d023839 show significantly higher expression in roots.

1005

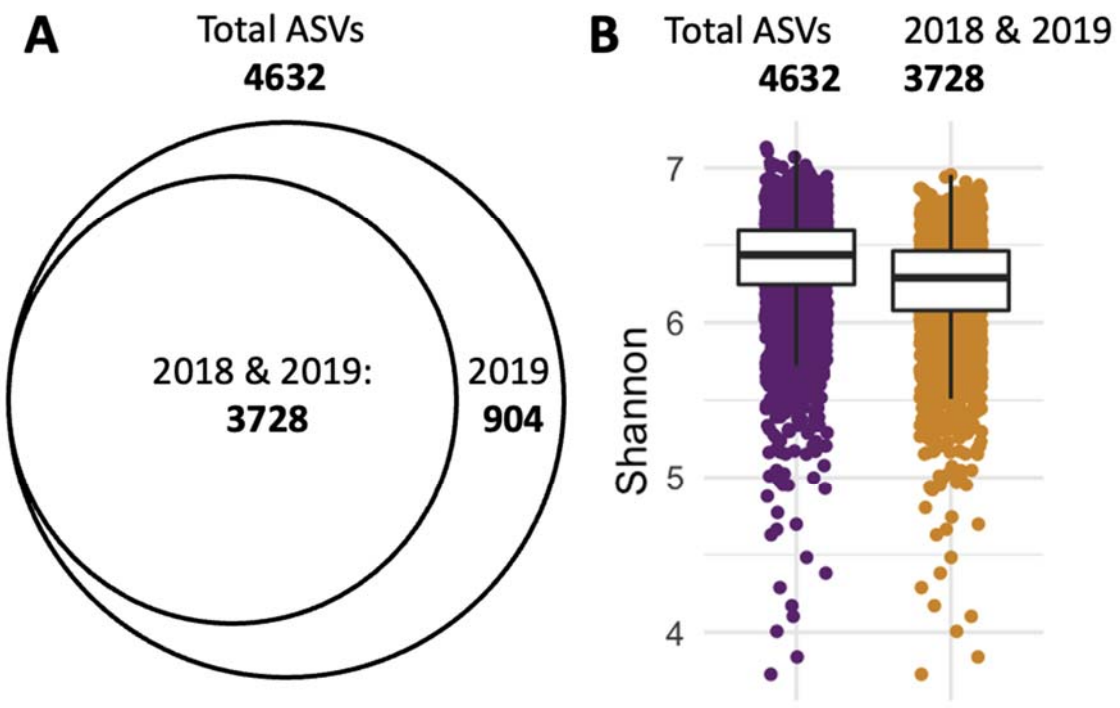

Figure 7 - figure supplement 1: **Retaining ASVs observed in both years reduces dataset complexity with minimal loss of diversity.** (A) Intermediate set of ASVs after prevalence filtering contains 4,632 ASVs, of which 904 were exclusively found in 2019. (B) Comparison of the Shannon diversity between the total set (4632 ASVs, purple) and the shared set (3728 ASVs, gold) reveals a 2.29% loss in diversity: Median(Shannon3728)/Median(Shannon4632) = 0.9771.

1006